



Review article

Catalytic reactions promoted by metal complexes stabilized by 1,3,5-triaza-7-phosphatricyclo[3.3.1.1]decane (PTA) and derivatives. A brief survey of recent results

Antonella Guerriero^{*}, Luca Gonsalvi^{*}

Consiglio Nazionale delle Ricerche (CNR), Istituto di Chimica dei Composti Organometallici (ICCOM), Via Madonna del Piano 10, 50019 Sesto Fiorentino (Florence), Italy

ABSTRACT

In this review article, we present a brief survey of the recent contributions (2018–2024) appeared in the scientific literature, describing the use of the cage-like water-soluble monodentate phosphine 1,3,5-triaza-7-phosphatricyclo[3.3.1.1]decane (also known as 1,3,5-triaza-7-phosphadamantane, PTA), some of its derivatives and a higher homologue as stabilizing ligands for precious and non-precious metal complexes, with various applications in homogeneous catalytic processes in water and biphasic media.

1. Introduction

Metal-catalyzed reactions are valuable approaches for chemical transformations, decreasing the overall energy demand of the processes. Research in catalysis has addressed over the years many different aspects connected to catalyst design and synthesis, process optimization, mildening reaction conditions, use of additives and cocatalysts, etc. In particular, homogeneous catalysis has the advantage of easier catalyst tunability compared to heterogeneous catalysis, and chemists can refer to a huge amount of literature on the synthesis of suitable molecular architecture, by subtle matching of (transition) metal precursors and appropriate stabilizing ligands that can impart the desired electronic and steric properties around the metal center of the organometallic or coordination complexes so obtained.

Over the years, with the aim of increasing environmental and economical sustainability, many research groups have studied the possibility to convey in more benign media some catalytic processes traditionally run in organic solvents, *i.e.* using aqueous-phase or biphasic water-organic solvent media, as water is a safer and green alternative to toxic organic solvents [1,2]. The use of hydrophilic ligands was demonstrated to be one of the most suitable approaches to achieve this goal [3]. A well-represented community of researchers, including ourselves, has gathered and often collaborated in the last 20 years to develop aqueous-phase catalysis using the neutral adamantane-like phosphine 1,3,5-triaza-7-phosphatricyclo[3.3.1.1]decane (also known as 1,3,5-triaza-7-phosphadamantane, PTA) and its derivatives [4], that

were generally obtained either by *N*-quaternization (lower rim functionalization) or by the introduction of an additional binding arm in C-6 position (upper rim functionalization) [5]. Other synthetic modifications of PTA include cage opening, giving novel ligands with a possible κ^2 -bidentate behavior either by P,N or N,N coordination, and more recently by expanding the size of the adamantane cage as in the higher PTA homologue 1,4,7-triaza-9-phosphatricyclo[5.3.2.1]tridecane (CAP) [6]. A huge variety of catalytic applications of transition metal complexes containing such ligands has been described and summarized in various review article.

The first comprehensive review on the synthetic coordination chemistry of PTA and its applications in catalysis, medicinal chemistry and luminescence studies was published by our group 20 years ago [4a]. Over the years, updates were made available by us and other research groups, focusing on specific aspects of the chemistry and applications of PTA and derivatives [4]. Recent reviews and book chapters have summarized the main results of the use of metal PTA complexes in the field of medicinal chemistry [7] and in the building of coordination networks [8]. To the best of our knowledge, only two review articles have appeared after 2018 on the topic of catalytic applications of this class of compounds, the first focusing on Ru complexes of PTA and other urotropine ligands [9] and the second on the comparison between PTA and CAP complexes [10], respectively. In this contribution, we present an updated survey of the main results in catalytic processes in the presence of precious- and non-precious metal complexes stabilized by PTA, CAP and other derivatives (Fig. 1), described in the literature in the period

^{*} Corresponding authors.

E-mail addresses: antonella.guerriero@iccom.cnr.it (A. Guerriero), l.gonsalvi@iccom.cnr.it (L. Gonsalvi).

<https://doi.org/10.1016/j.ica.2024.122295>

Received 20 June 2024; Received in revised form 30 July 2024; Accepted 30 July 2024

Available online 3 August 2024

0020-1693/© 2024 The Author(s). Published by Elsevier B.V. This is an open access article under the CC BY license (<http://creativecommons.org/licenses/by/4.0/>).

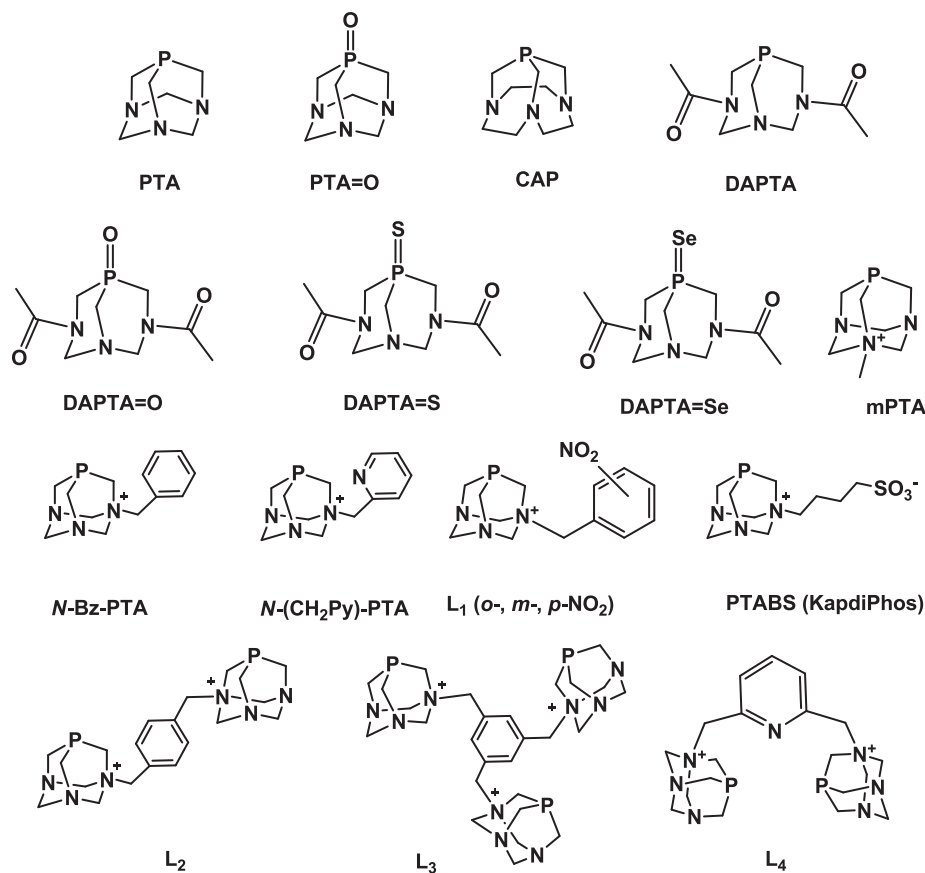
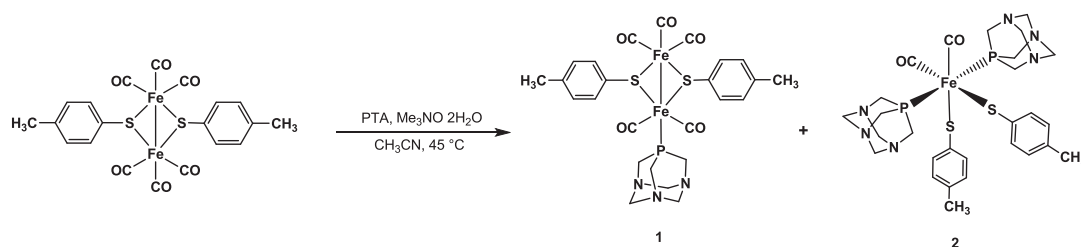


Fig. 1. Molecular drawings of PTA, its neutral open-cage and lower-rim cationic derivatives, and the higher homologue CAP hereby discussed.



Scheme 1. Synthesis of Fe-PTA complexes **1** and **2**.

2018–2024. Other complexes, obtained in this period and used for other type of applications, will not be hereby discussed.

2. Catalytic applications of non-precious metal-PTA complexes

In recent years, the growing concern on economic and environmental sustainability of chemical processes has driven research to find solutions to replace costly precious metal catalyst with non-precious, earth-abundant counterparts. In the case of PTA-type complexes, some studies were reported involving metals such as Fe, Mn, Cu and Sn, and the main features in catalytic applications are hereby summarized.

2.1. Iron

The synthesis of dinuclear and mononuclear iron complexes $[\text{Fe}_2(\mu\text{-SC}_6\text{H}_4\text{CH}_3\text{-}p)_2(\text{CO})_5(\text{PTA})]$ (**1**) and $[\text{Fe}(\kappa^1\text{-SC}_6\text{H}_4\text{CH}_3\text{-}p)_2(\text{CO})_2(\text{PTA})_2]$ (**2**) was reported by Agarwal and Kaur-Ghumaan in 2020 [11]. These complexes were obtained in acetonitrile by reacting the diiron hexacarbonyl precursor $[\text{Fe}_2(\mu\text{-SC}_6\text{H}_4\text{CH}_3\text{-}p)_2(\text{CO})_6]$ with PTA in the

presence of $\text{Me}_3\text{NO}\cdot 2\text{H}_2\text{O}$ and purified by silica gel column chromatography (Scheme 1). Complex **1** was obtained as the major product in ca. 32 % yield, while **2** was obtained in very low yield (ca. 11 %). Both compounds were tested as catalysts in the electrocatalytic hydrogen reduction (HER) process. The cyclic voltammograms (CVs) were measured under argon in acetonitrile and in dichloromethane at a scan rate of 0.1 Vs^{-1} . One-electron reductions were observed with complex **1** at -1.66 and -1.92 V in CH_3CN and at -2.06 V in DCM. Complex **2** showed irreversible one-electron reductions at -1.75 and -1.97 V in acetonitrile and as **1**, **2** displayed irreversible oxidations in CH_3CN . In addition, the CVs of the two iron complexes in the presence of different acids as proton sources were measured again in acetonitrile and dichloromethane. In CH_3CN , the dinuclear compound **1** was active in the electrocatalytic proton reduction with trifluoroacetic acid (TFA) but showed no catalytic activity in the presence of acetic acid (AA) in the same solvent. On the other hand, **3** showed proton reduction at -2.29 V in DCM by using AA. Mononuclear complex **2** was active with AA in CH_3CN but decomposed in the presence of stronger acids.

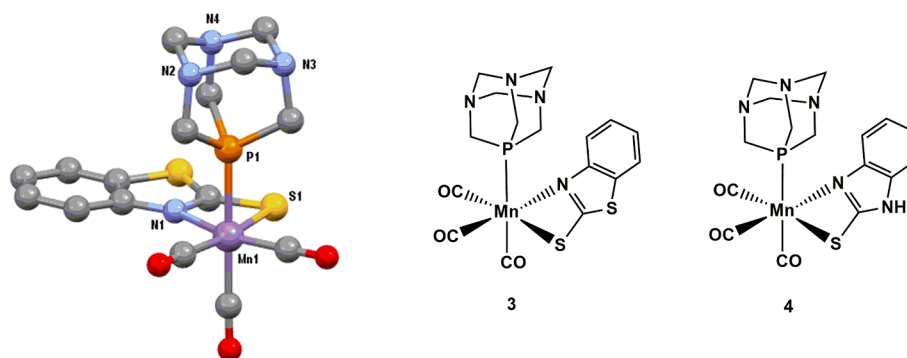


Fig. 2. Molecular drawings of complexes **3** and **4** and X-ray crystal structure of **3** (hydrogen atoms omitted for clarity, drawing by CCDC Mercury® 3.9) [13].

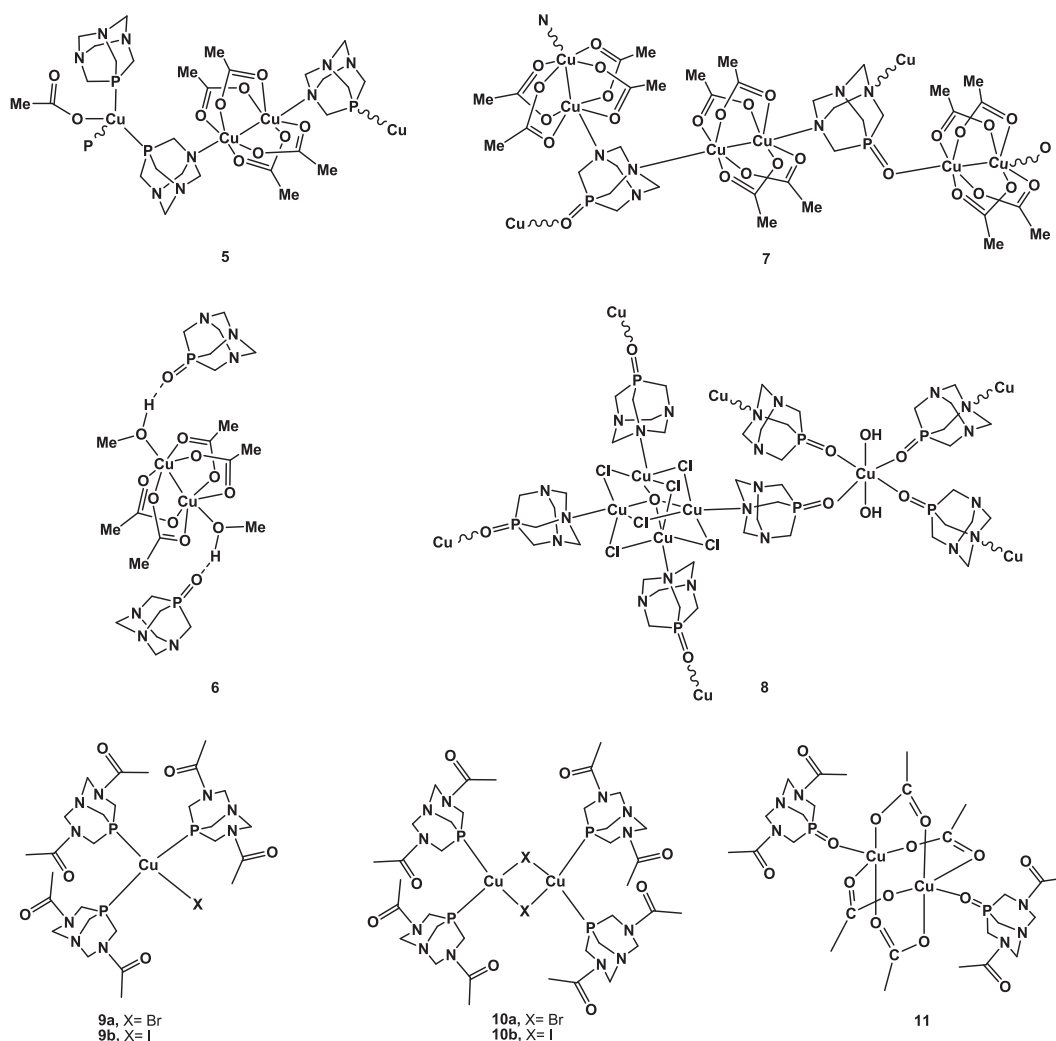
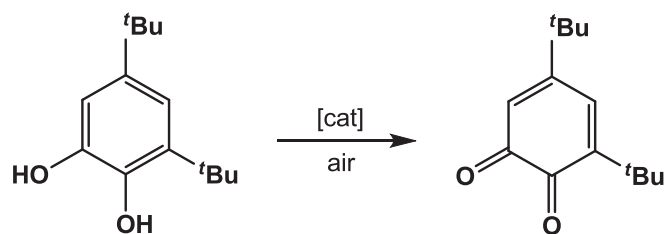


Fig. 3. Molecular drawings of Cu-PTA (**5**), Cu-PTA=O (**6–8**), Cu-DAPTA (**9–10**) and Cu-DAPTA=O (**11**) compounds.

2.2. Manganese

Although most of the coordination complexes of PTA with group 7 elements are those of rhenium and technetium often aimed for radiopharmaceutical applications, some manganese complexes bearing P-bound PTA ligand have also been reported [12]. Recently, the two mononuclear Mn(I) complexes *fac*-[Mn(CO)₃(κ²-S₂NC₇H₄)(PTA)] (**3**) and *fac*-[Mn(CO)₃(κ²-SN₂C₇H₅)(PTA)] (**4**), shown in Fig. 2, were synthesized by reaction of dinuclear manganese precursors [Mn₂(CO)₆(μ-

S₂NC₇H₄)₂] and [Mn₂(CO)₆(μ-SN₂C₇H₅)₂] with PTA in dichloromethane at room temperature and in air [13]. In addition to FTIR, NMR and ESI-MS characterization techniques, single-crystal X-ray diffraction data were obtained for complex **3**, revealing that the N and S atoms of 2-mercaptobenzothiazole ligand and two carbonyl groups occupy the equatorial plane around the metal center, whereas the P atom of PTA and one carbonyl group are in axial positions with respect to manganese (Fig. 2). Complexes **3** and **4** were found to be active for electrocatalytic proton reduction in both organic (CH₃CN) and aqueous/organic media



Scheme 2. Catalytic oxidation of 3,5-di-*tert*-butylcatechol (3,5-DTBC) to 3,5-di-*tert*-butyl-*o*-benzoquinone (3,5-DTBQ).

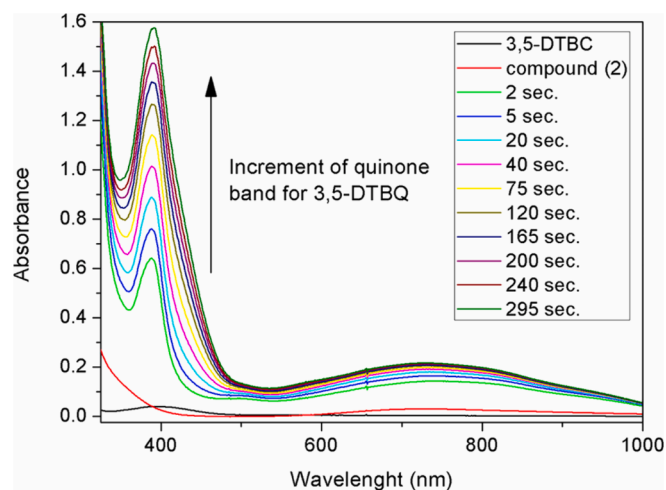


Fig. 4. UV-vis spectrum showing the adsorption band of 3,5-DTBQ (at 390 nm) derived from the catalytic oxidation of 3,5-DTBC (1.33×10^{-2} M) in MeOH in the presence of compound 9 (6.50×10^{-5} M). Reprinted with permission from [14], copyright @ 2018 American Chemical Society.

($\text{CH}_3\text{CN}/\text{H}_2\text{O}$, 1:1), using trifluoroacetic acid and acetic acid as proton sources. In particular, **3** catalyzed the reaction at a more positive potential than complex **4** and showed very good turnover frequency (TOF/ s^{-1}) (O.P., η/V) of 718 s^{-1} (1.11) in CH_3CN and a TOF of 280 s^{-1} in the $\text{CH}_3\text{CN}/\text{H}_2\text{O}$ mixture.

2.3. Copper

The self-assembly synthesis of copper coordination compounds driven by PTA or derivatives is one among the most interesting topics widely investigated by the two research groups of Smoleński and Pombeiro. By reacting copper(II) acetate with PTA in the presence of metallic copper(0) powder in MeCN under reflux conditions, the 1D coordination polymer $[\text{Cu}_3(\mu\text{-MeCOO})_4(\text{MeCOO})(\mu\text{-PTA})_2(\text{PTA})]_n$ (**5**) has been obtained (Fig. 3) [14]. This compound represents a rare example of a mixed valence Cu(II)/Cu(I) PTA-based polymer wherein, as revealed by the corresponding X-ray crystal structure, the phosphine moieties are at the same time P,*N*-linkers and terminal P-bound ligands. When the oxide derivative PTA=O was used instead of PTA, the reaction with Cu(MeCOO)₂ in methanol at room temperature produced the zero-dimensional (0D) dicopper(II) compound of formula $[\text{Cu}_2(\mu\text{-MeCOO})_4(\text{MeOH})_2](\text{PTA}=\text{O})$ (**6**). A slight variation of the reaction conditions, *i.e.* by refluxing PTA=O and Cu(MeCOO)₂ in MeCN, led to the formation of the 3D copper(II) MOF (metal-organic framework) $[\text{Cu}_3(\mu\text{-MeCOO})_6(\mu_3\text{-PTA}=\text{O})_2]_n \cdot 3.5n \text{ MeCN}$ (**7**) (Fig. 3). The solid-state molecular structures of **6** and **7** were established by X-ray diffraction showing that in **7** PTA=O acts as an unusual tridentate N,N,O ligand and the μ_3 -PTA=O spacers are connected to axial positions of Cu centers, whereas in **6** the axial positions of metal centers are occupied by MeOH molecules and two phosphine oxide moieties are H-bonded to a dicopper

(II) unit. Magnetic properties of all these three coordination compounds were also investigated disclosing a strong antiferromagnetic interaction between copper atoms within the Cu_2 blocks.

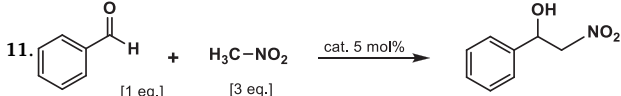
The highly air-stable compounds **6** and **7** were tested as catalysts in the aerobic oxidation of 3,5-di-*tert*-butylcatechol (3,5-DTBC) to the corresponding diketone 3,5-di-*tert*-butyl-*o*-benzoquinone (3,5-DTBQ), chosen as model test reaction for catechols oxidation (Scheme 2). The catalytic activity was performed under homogeneous conditions in methanol at room temperature and the product formation was monitored by UV-vis spectroscopy. Fig. 4 shows the increment of the adsorption band of 3,5-DTBQ (390 nm) in the presence of **7**. The catalytic turnover frequencies (k_{cat}), measured as $V_{\text{max}}/[\text{catalyst}]$, resulted 49.62 and 80.92 min^{-1} for **6** and **7** respectively, at values higher than those determined for Cu(MeCOO)₂ (20.88 min^{-1}) under the same conditions [14].

Some years later, Smoleński, Kirillov and coworkers reported the formation of another Cu(II)-PTA=O based 3D metal-organic framework of formula $[\text{Cu}_4(\mu\text{-Cl})_6(\mu_4\text{-O})\text{Cu}(\text{OH})_2(\mu\text{-PTA}=\text{O})_4]_n \cdot 2n \text{ Cl-EtOH} \cdot 2.5n \text{ H}_2\text{O}$ (**8**) (Fig. 3). This was generated in the self-assembly reaction of copper(II) nitrate and PTA=O in a 2-chloroethanol/ethanol (1:1) mixture, during which the formation of the intermediate $[\text{H-PTA}=\text{O}]_2[\text{CuCl}_3(\text{NO}_3)]$ (where H-PTA=O is the *N*-protonated form of the ligand) was observed [15]. MOF complex **8** was employed as an efficient catalyst for the oxidation and hydrocarboxylation of alkanes to alcohols and ketones or carboxylic acids under mild conditions. In particular, **8** catalyzed the oxidation of propane (1 atm) at 50°C achieving a total yield of 14 % (based on propane) after 5 h, giving isopropyl alcohol and acetone as the main products of oxidation. The highest TON=280 (TON = turnover number, calculated as moles of products/moles of catalyst) was obtained when the substrate pressure was increased to 8 atm and, in contrast to numerous Cu-catalyzed systems applied in the same oxidation reaction, the addition of an acid promoter was not required with this coordination compound. This feature was observed also in the oxidation of cyclohexane catalyzed by **8** (resulting in ca. 15 % yields of cyclohexanol and cyclohexanone) where the addition of TFA (trifluoroacetic acid), that is often used as a promoter of Cu-based catalytic systems, did not affect the catalytic performance. Moreover, **8** resulted to be an active catalyst in the hydrocarboxylation of cyclohexane to cyclohexanecarboxylic acid (30 % yield) and of propane to isobutyric acid (22 % yield) and *n*-butyric acid (6.2 % yield) in an aqueous/acetonitrile solution at 60°C [15].

In a series of collaborative works carried out by the research groups of Smoleński and Pombeiro, copper complexes bearing 3,7-diacetyl-1,3,7-triaza-5-phosphabicyclo[3.3.1]nonane (DAPTA) and its derivatives (Fig. 1) as coordinating ligands were described. DAPTA is the di-*N*-acetylated product of PTA, belonging to the family of the open-cage derivatives and, like PTA, shows high solubility in water. Mononuclear complexes of formula $[\text{CuX}(\text{DAPTA})_3]$ (**7a**, X = Br; **7b**, X = I) and dinuclear $[\text{Cu}(\mu\text{-X})(\text{DAPTA})_2]_2$ complexes (**10a**, X = Br; **10b**, X = I) (Fig. 3) were obtained by reacting Cu(I)-halide (bromide or iodide) with the phosphine in a mixture of acetonitrile and ethanol at room temperature [16]. All these compounds were isolated as air stable white colored powders and, with the exception of **10b**, they resulted soluble in water and in polar organic solvents, such as acetonitrile, dichloromethane and DMSO. Compounds **9–10** were tested as catalysts in the three-component 1,3-dipolar cycloaddition reaction (CuAAC) of terminal alkynes with *in situ* generated azides to afford the corresponding 1,4-disubstituted 1,2,3-triazoles. The products precipitated from the mother liquor solutions and were easily separated by filtration. The reactions were carried out in a water/acetonitrile 1:1 mixture, under microwave irradiation (30 W), at 125°C and for 15 min. Although all complexes resulted active in the CuAAC “click” reaction of phenylacetylene, benzyl bromide and sodium azide to produce 1-benzyl-4-phenyl-1*H*-1,2,3-triazole, compound $[\text{Cu}(\text{DAPTA})_3]$ (**9b**) was found to be the most active catalyst, giving yields in the range 75–99 % depending on the catalyst loading. In recycling tests, when 5 mol%

Table 1

Henry reaction of benzaldehyde with nitromethane (top) and nitroethane (bottom) catalyzed by complex

11. 

Catalyst	Time (h)	Temperature (°C)	Solvent (2 mL)	Yield ^a [%]	TON ^b
11	48	75	H ₂ O	91	18
11	60	75	H ₂ O	94	19
11	48	60	EtOH	97	20
11	48	60	H ₂ O/EtOH (1:1)	96	19
11 ^c	24	23	H ₂ O	>99	20

Catalyst	Time (h)	Temperature (°C)	Selectivity ^a (anti/syn)	Yield ^a [%]	TON ^b
11	48	75	30:70	83	17
11	60	75	29:71	88	18
11 ^c	24	23	49:51	87	18

^a Determined by analysis of the crude product by ¹H NMR spectroscopy.^b Turnover number calculated as number of moles of product per moles of catalyst.^c In the presence of trimethylamine (5 mol%).

catalyst were used under the reaction conditions described above, **9b** showed a high catalytic activity during the first two cycles but a significant decrease of its activity from the third cycle [16]. Catalyst **9b** was also tested in the azide-alkyne cycloaddition reaction (CuAAC) of benzyl bromide and sodium azide with different alkynes, and the best result in terms of yield of the corresponding 1,2,3-triazole was obtained with 1,4-diethynylbenzene, affording the corresponding bis-triazole in 97 % yield.

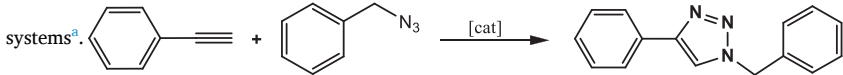
The catalytic oxidation of 3,5-di-*tert*-butyl-catechol (3,5-DTBC) to 3,5-di-*tert*-butyl-*o*-benzoquinone (3,5-DTBQ) (Scheme 1) was again investigated by the same research groups by using the dinuclear copper (II) complex [Cu(μ-CH₃COO)₂(κO-DAPTA=O)]₂ (**11**) as catalyst (Fig. 3), where DAPTA=O is the phosphine oxide derivative of DAPTA (Fig. 1) [17]. This oxide is usually prepared in two steps reaction consisting first in the oxidation of PTA to PTA=O, followed by the acetylation of the latter with acetic anhydride in water [18]. In the case of **11**, the formation of DAPTA=O was obtained together with the complex by reacting DAPTA and Cu(II) acetate monohydrate in air and in a wet mixture of toluene and ethanol. In comparison with other dinuclear

acetate-bridging copper(II) complexes, **11** showed higher activity and better efficiencies in the catalytic oxidation of 3,5-DTBC to the corresponding quinone and, by means of theoretical DFT studies, a mechanism of the catalytic cycle was proposed by the authors. The cycle involved the cooperation of the acetate ligands connected to copper and the interaction of the catechol substrate with only one of the metal centers during the oxidation process.

Complex **11** was also tested as catalyst in the nitroaldol coupling (Henry reaction) of benzaldehyde with nitromethane and nitroethane under aqueous homogeneous conditions (Table 1) [17]. In the reaction with nitromethane, the product 1-phenyl-2-nitroethanol was obtained in 94 % yield after 60 h by using 5 mol% of the catalyst in water at 75 °C, while the conversion resulted quantitative after 24 h by running the reaction at room temperature in the presence of catalytic amount of triethylamine. When the reaction was performed in ethanol or in a water/ethanol mixture (1:1), conversions of 97 % and 96 % respectively, were observed after 48 h at 60 °C temperature (Table 1). By using nitroethane instead of nitromethane with benzaldehyde, the nitroaldol coupling reaction catalyzed by complex **11** produced the *anti* and *syn*

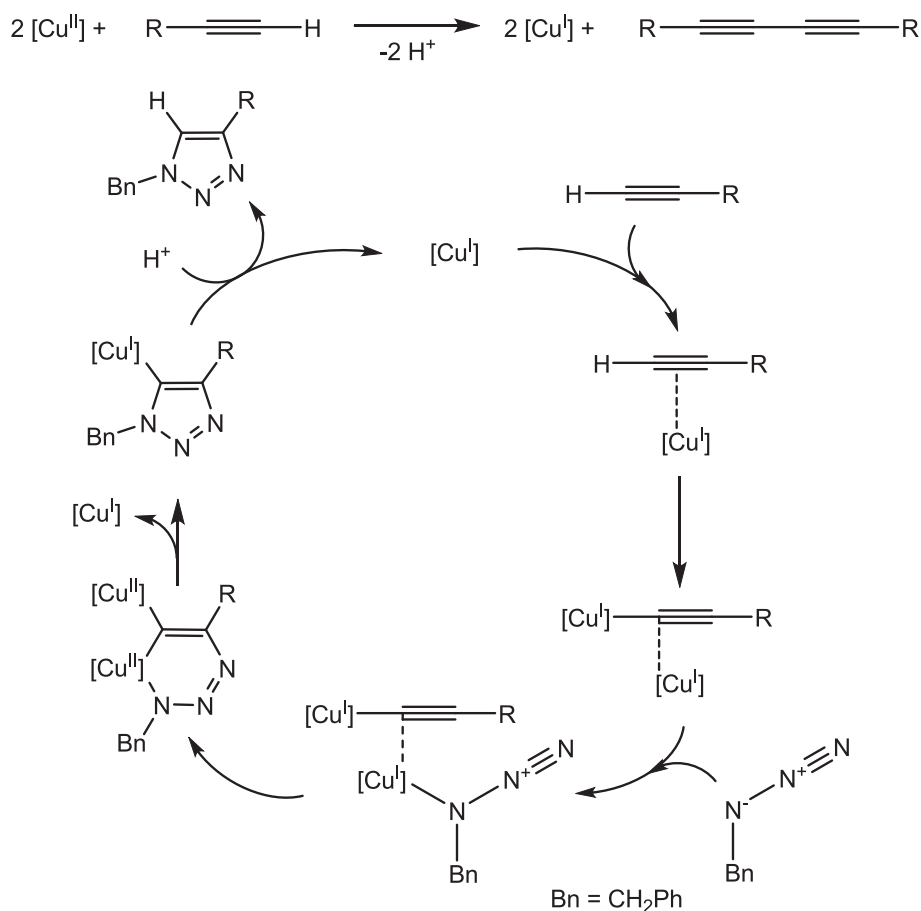
Table 2

Copper-catalyzed azide-alkyne cycloaddition (CuAAC) reaction of phenylacetylene and benzyl azide catalyzed by different catalytic

systems^a. 

Entry	Catalytic system	Solvent	Time (h)	T (°C)	Isolated Yield ^c [%]
1	CuI/ DAPTA=O ^b	H ₂ O	24	25	62
2	Cu(CH ₃ COO) ₂ /DAPTA=O ^b	H ₂ O	24	25	73
3	Cu(CH ₃ COO) ₂ /DAPTA=O ^b	H ₂ O/MeOH (1:1)	24	25	69
4	Cu(CH ₃ COO) ₂ /DAPTA=O ^b	H ₂ O/EtOH (1:1)	24	25	75
5	Cu(CH ₃ COO) ₂ /DAPTA=O ^b	H ₂ O/ ^t BuOH (1:1)	24	25	78
6	Cu(CH ₃ COO) ₂ /DAPTA=O ^b	H ₂ O/DMF (1:1)	24	25	88
7	Cu(CH ₃ COO) ₂ /DAPTA=O ^b	H ₂ O/MeCN (1:1)	24	25	97
8	Cu(CH ₃ COO) ₂ /DAPTA=O ^b	H ₂ O/MeCN (1:1)	8	80	>99
9	11 (2 mol%)	H ₂ O/MeCN (1:1)	24	25	93
10	11 (5 mol%)	H ₂ O/MeCN (1:1)	24	25	>99
11	11 (1 mol%)	H ₂ O/MeCN (1:1)	48	25	88
12	11 (1 mol%)	H ₂ O/MeCN (1:1)	6	80	>99

^a Reaction conditions: phenylacetylene (1 mmol), benzyl azide (1 mmol), solvent (3 mL).^b CuI or Cu(CH₃COO)₂·H₂O (1 mol%), DAPTA=O (2 mol%).^c Triazoles were isolated by filtration, washed and dried.



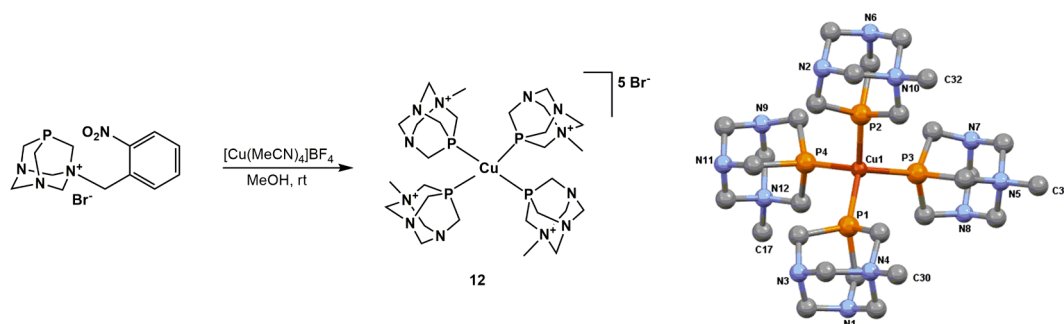
Scheme 3. Proposed catalytic cycle for the CuAAC reaction in the presence of **11** [19].

diastereoisomers of 1-phenyl-2-nitropropanol (Table 1). In aqueous medium at 75 °C, conversions of 83 % and 88 % were achieved with 5 mol% of **11** after 48 h and 60 h, respectively, in both cases with higher selectivity towards the *syn* isomer. As in the reaction with nitromethane, the presence of triethylamine led to a better catalytic performance achieving a conversion of 87 % after 24 h at room temperature. The catalytic activity of **11** was further investigated in the nitroaldol reaction of numerous *para*-substituted aromatic aldehydes to give the corresponding β -nitro alcohols, resulting in yields ranging from 51 to 97 % depending on the aldehydes. Higher reactivities were typically observed in the presence of aldehydes bearing an electron-withdrawing group (nitro, bromo, or chloro group). In the same work, the authors described also the results of the catalytic performances of **11** in the aerobic oxidation of benzyl alcohol mediated by TEMPO (2,2,6,6-tetramethylpiperidin-1-oxyl radical) to produce benzaldehyde. All reactions were run in 0.1 M aqueous solution of K₂CO₃ at 80 °C, reaching the highest conversion of 89 % with 5 mol% of compound **11** after 48 h [17].

Further catalytic applications of complex [Cu(μ -CH₃COO)₂(κ O-DAPTA=O)]₂ (**11**) and the synthetic modification of DAPTA ligand, as well as the catalytic activity of its corresponding derivatives in the presence of copper salts, were investigated by Smoleński, Pombeiro and coworkers in a more recent research work [19]. First, the authors described a new synthetic procedure to obtain DAPTA=O, consisting in the direct oxidation of DAPTA with hydrogen peroxide in ethanol at 0 °C. The corresponding sulfide and selenide derivatives of the diacetyl phosphine, *i.e.* DAPTA=S and DAPTA=Se (Fig. 1), were also synthesized by reacting DAPTA with sulfur or selenium in methanol under ultrasonic irradiation. As the original phosphine, all these derivatives maintained a high solubility in water. The observation of four resonances for the acyl groups in the ¹H NMR spectra and of three signals in the ³¹P{¹H}NMR

spectra of DAPTA=O or DAPTA=S or DAPTA=Se in different deuterated solvents, were indicative of the existence in solution of three rotamers for each phosphine, *i.e.* the *syn* (ZZ), the *syn* (EE) and the *anti* (ZE) forms. As for the Cu-DAPTA halide complexes described above, phosphines DAPTA=O, DAPTA=S and DAPTA=Se were tested in CuAAC reaction of phenylacetylene and benzyl azide in combination with several Cu(I) and Cu(II) salts. The catalytic experiments were performed in water at room temperature under air for 24 h in the presence of 1 mol% of Cu salt and 2 mol% of DAPTA derivative. Under these conditions, compared to DAPTA=S and DAPTA=Se, DAPTA=O showed better catalytic activity, yielding the triazole in 62 % and in 73 % in combination with CuI or Cu(CH₃COO)₂·H₂O, respectively (Table 2, entries 1 and 2). Conversions ranging from 69 to 97 % were obtained when the tests were carried out with the *in situ* generated catalyst from Cu(CH₃COO)₂·H₂O (1 mol%) and DAPTA=O (2 mol%) in mixtures of water and water-miscible organic solvents (MeOH, EtOH, ^tBuOH, DMF, MeCN) and the quantitative yield was achieved performing the reaction in H₂O/MeCN (1:1) mixture at 80 °C for 8 h (Table 2, entry 8). By considering the results showed by the system Cu(CH₃COO)₂·H₂O/DAPTA=O, complex **11** was also tested in the same CuAAC reaction (Table 2, entries 9–12). The effects of catalyst loading, time and temperature on the catalytic performance of **11** were investigated and the reaction reached completion in the conditions indicated in entries 10 and 12 of Table 2. Cu(CH₃COO)₂·H₂O/DAPTA=O system and complex **11** resulted also active as catalysts in the one-pot synthesis of different 1,4-disubstituted-1,2,3-triazoles by reacting benzyl azide with several *meta*- or *para*-substituted phenylacetylenes, but both catalytic systems exhibited very poor recyclability with a drop on triazoles production from the second cycle [19]. The proposed catalytic cycle for the CuAAC reaction is shown in Scheme 3.

Among the new Cu-PTA compounds used in catalysis, a new series of



Scheme 4. Synthesis of complex $[\text{Cu}(\text{mPTA})_4]\text{Br}_5$ (**12**) and its X-ray crystal structure (hydrogen atoms, solvent molecules and anions omitted for clarity, drawing by CCDC Mercury® 3.9) [20].

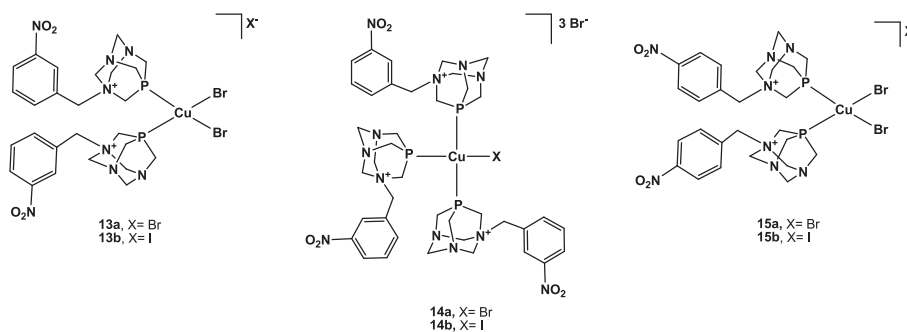
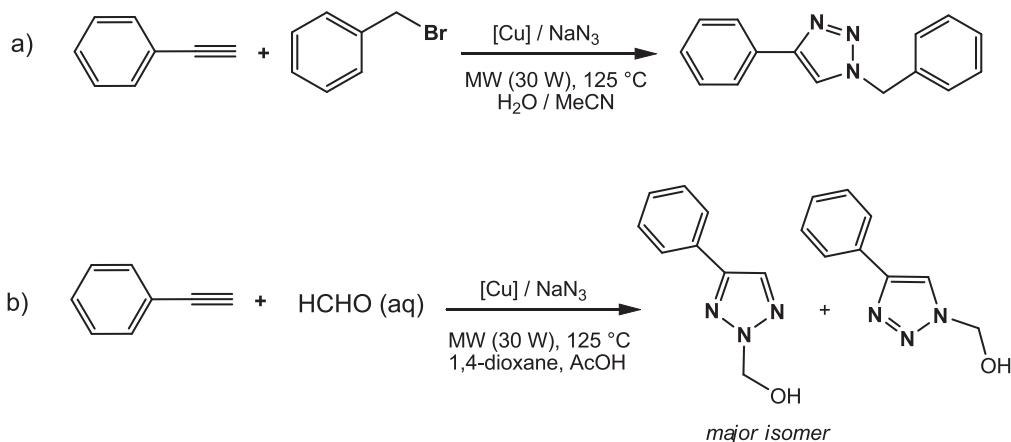


Fig. 5. Molecular drawings of Cu(I) complexes **13–15** [20].

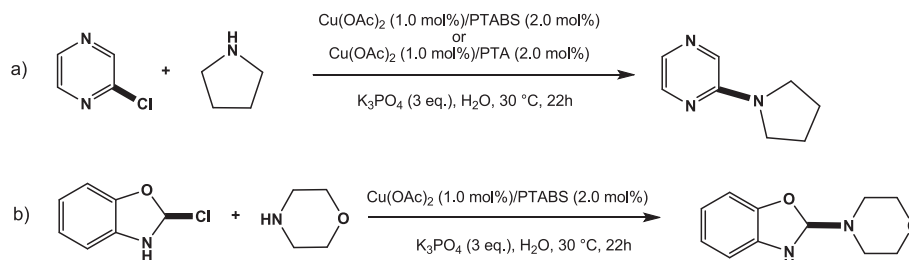


Scheme 5. Cu-catalyzed cycloaddition reaction of a) phenylacetylene, benzyl bromide and sodium azide and b) phenylacetylene, formaldehyde and sodium azide under microwave irradiation.

copper(I) complexes bearing certain *N*-alkylated PTA derivatives were reported some years ago [20]. The reaction of $[\text{Cu}(\text{MeCN})_4]\text{BF}_4$ with both a stoichiometric amount or a four-fold excess of ligand [*o*-NO₂-benzyl-PTA]Br (*o*-L₁, Fig. 1) in methanol at room temperature afforded the Cu(I) complex of formula $[\text{Cu}(\text{mPTA})_4]\text{Br}_5$ (**12**) (mPTA=*N*-methyl-1,3,5-triaza-7-phosphadamantane, Scheme 4). Besides several techniques of characterization in solution, the molecular structure of **12** in the solid state, characterized by a Cu-centred tetrahedron with P-bound ligands at the apexes, was identified by X-ray diffraction of single crystals produced by the slow evaporation in air of the mother liquor (Scheme 3). The formation of a final complex containing mPTA instead of the *N*-Bz-PTA, upon C–C bond cleavage in the starting *o*-nitro-benzylated ligand under reaction conditions, was attributed by the authors to the high steric hindrance of the NO₂ group in *ortho* position. On the other hand, copper-catalyzed C–C bond cleavage from *N*-(*n*-butyl)PTA

to mPTA was previously described [21], thus a similar mechanism cannot be ruled out also for the present case.

When the *meta*- or *para*-nitrobenzyl-PTA derivatives *m*-L₁ and *p*-L₁ were reacted with CuBr or CuI in 1:2 or 1:4 ratios, the six compounds **13–15** were obtained (Fig. 5). Copper complexes **12–15** were screened as homogeneous catalysts in the cycloaddition reaction of phenylacetylene, benzyl bromide and sodium azide under microwave irradiation (Scheme 5). Based on the catalytic tests previously optimized with Cu-DAPTA complexes [16], the same conditions were applied, *i.e.* catalyst loading of 3 mol%, 125 °C, irradiation of 30 W and 1.5 mL of water/acetonitrile (1:1) mixture. Compound $[\text{CuBr}_2(\text{m-L}_1)_2]\text{I}$ (**13b**) showed the highest catalytic activity under these conditions, affording 1-benzyl-4-phenyl-1*H*-1,2,3-triazole in 47 % yield after 15 min. The conversion further increased to 84 % when the total volume of the H₂O/MeCN mixture was reduced to 1 mL, and up to 99 % by using a volume of

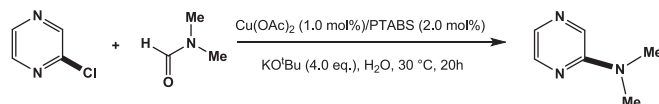


Scheme 6. Selected coupling reactions catalyzed by Cu(II)/PTABS system [22].

0.5 mL and a total time of reaction of 1 h. With a catalyst loading of 3 mol%, 125 °C and irradiation of 30 W, the one-pot three-component CuAAC reaction was then carried out in the presence of **13**–**15** by replacing benzyl bromide with formaldehyde in 1,4-dioxane under slightly acidic conditions. In this case, complex $[\text{CuBr}_2(m\text{-L}_1)_2]\text{Br}$ (**13a**) resulted the best catalyst producing a 36 % yield of the regioisomeric mixture of 2- and 1-hydroxymethyl-4-phenyl-1,2,3-triazole, with the former as the major isomer. By using a $\text{H}_2\text{O}/\text{dioxane}$ (2:1) mixture instead of neat dioxane, yields of 73 % and 88 % were obtained after 15 and 60 min respectively, in the presence of the same copper catalyst.

The heterogenization of compounds $[\text{CuBr}_2(m\text{-L}_1)_2]\text{Br}$ (**13a**) and $[\text{CuBr}_2(m\text{-L}_1)_2]\text{I}$ (**13b**) by immobilization on activated carbon materials (AC) or carbon nanotubes (CNT) and their use in the one-pot three-component (phenylacetylene, benzylbromide, sodium azide) CuAAC reaction, was also reported in the same article [20]. In detail, copper complex **13b** immobilized on different types of carbon supports was used as heterogeneous catalyst for this reaction and the system **13b**_CNT-ox-Na (where CNT-ox-Na is a multi-walled carbon nanotube material oxidized with HNO_3 and then treated with NaOH) gave the best results in terms of conversion to the corresponding triazole (*i.e.* 1-benzyl-4-phenyl-1*H*-1,2,3-triazole). The recyclability of this system was assessed in six consecutive runs, showing a drastic drop of the catalytic activity after the first cycle probably due to the catalyst leaching. System **13b**_CNT-ox-Na was then tested in the reaction of various substituted benzyl bromides with phenylacetylene or 1,4-diethynylbenzene again under microwave irradiation, producing the corresponding triazoles in yields ranging from 29 to 80 %. $[\text{CuBr}_2(m\text{-L}_1)_2]\text{Br}$ (**13a**) was also immobilized on carbon materials and the system **13a**_CNT-ox-Na was selected as heterogeneous catalyst for the synthesis of *N*-hydroxymethyl-1,2,3-triazoles by the three-component (phenylacetylene, formaldehyde, sodium azide) CuAAC reaction. Contrary to what observed with the system **13b**_CNT-ox-Na, **13a**_CNT-ox-Na resulted active in catalyst recycling tests, maintaining high activity for five consecutive cycles. Indeed, a total product yield of 78 % of the regioisomeric mixture of 1- and 2-hydroxymethyl-4-phenyl-1,2,3-triazoles was reached in the fifth cycle (reaction conditions: catalyst 2.5 mol%, $\text{H}_2\text{O}/1,4\text{-dioxane}$ 2:1, 30 W, 125 °C, 1 h).

Very recently, Kapdi and coworkers extensively explored the use of a copper-based system with the *N*-alkylated and sulfonated PTA derivative 4-(1,3,5-triaza-7-phosphaadamantan-1-ium-1-yl)butane-1-sulfonate (PTABS, also known as KapdiPhos, Fig. 1) in the catalytic amination of chloroheteroarenes with primary and secondary amines [22]. The catalyst was obtained *in situ* by $\text{Cu}(\text{OAc})_2 \cdot \text{H}_2\text{O}$ (1.0 mol %) in combination with PTABS (2.0 mol %) as stabilizing ligand and K_3PO_4 as the base. The product of the coupling reaction of 2-chloropyridine with pyrrolidine was obtained in 84 % yield (Scheme 6a). The catalytic reaction was carried out in neat water at 30 °C and, when performed in the presence of the system $\text{Cu}(\text{OAc})_2/\text{PTA}$, the yield of product reaction was only 61 %. The optimized catalytic conditions with Cu(II)/PTABS system were then employed in the amination of several chloroheteroarenes with primary amines as well as secondary amines, some of which were in the class of the active pharmaceutical intermediates (APIs). Good to excellent yields and high-purity products (>95 % HPLC purity) were



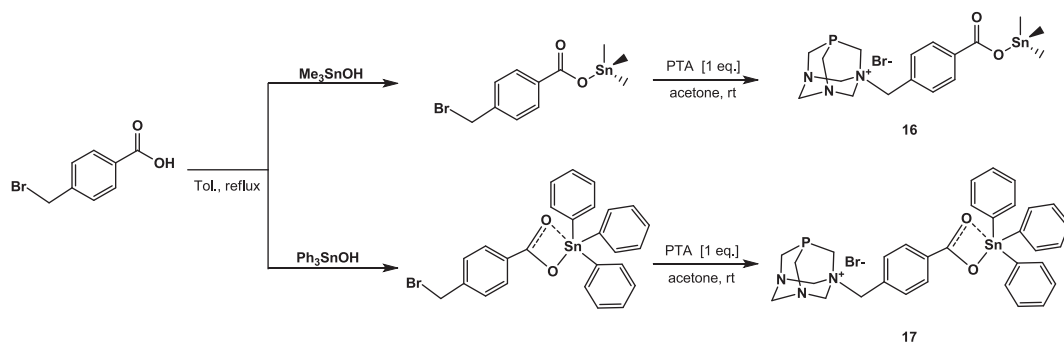
Scheme 7. *N,N*-dimethylation of 2-chloropyridine with DMF catalyzed by Cu(II)/PTABS system [23].

obtained in most cases. In particular, the coupling of 2-chlorobenzoxazole with morpholine (Scheme 6b) proceeded in nearly quantitative yield (99 %) with Cu(II)/PTABS and an excellent catalyst recyclability was displayed by this system, with no decrease of the catalytic activity for up to 12 consecutive cycles. Furthermore, when the reaction of 2-chlorobenzoxazole with morpholine was performed using various catalyst poisoning experiments, such as with the addition of Hg drops, the activity of Cu(II)/PTABS system was unaffected proving the homogeneity of the catalytic system.

The Cu(II)/PTABS system was further tested by the same research group in the catalytic dialkylation of chloroheteroarenes to produce amine-derivatized heteroaryl compounds [23]. In detail, reaction of 2-chloropyridine and *N,N*-dimethylformamide (DMF) with $\text{Cu}(\text{OAc})_2 \cdot \text{H}_2\text{O}$ (1.0 mol%) and several phosphines (2.0 mol%) in the presence of KO^tBu and water as additive was used as model test reaction (Scheme 7). As in the case of the coupling reactions described above, PTABS resulted the best ligands, and the Cu/PTABS system gave an almost quantitative yield of the desired product (95 %) and a higher catalytic activity compared to PTA (90 %). The Cu(II)/PTABS system was also investigated in the incorporation of the diethylamino functionality to numerous chloroheteroarenes using *N,N*-dimethylformamide as the precursor, giving the dialkylated products in yields ranging from 50 to 74 %. Finally, the Cu(II)/PTABS catalytic protocol was extended to different chloropurines and to the synthesis of commercially interesting drugs showing in all cases very good yields of the desired products.

2.4. Tin

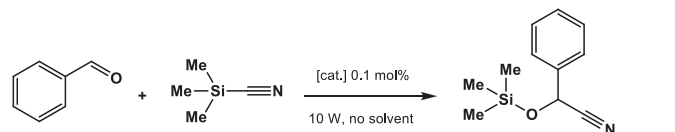
To complete the overview on the recently reported metal compounds of PTA and derivatives with non-precious metals with applications in catalysis, two novel tin(IV) complexes described by Mahmoud, Paul, Carabineiro and coworkers need to be mentioned, albeit metal coordination does not occur *via* PTA donor atoms. The preparation of the cationic complexes of general formula $[(\text{PTA}-\text{CH}_2-\text{C}_6\text{H}_4\text{-}p\text{-COO})\text{SnR}_3]\text{Br}$ (**16**, $\text{R}=\text{Me}$; **17**, $\text{R}=\text{Ph}$) involved a two-step process, consisting first in the synthesis of two bromomethylenebenzoate tin(IV) compounds which were then reacted with PTA in acetone at room temperature (Scheme 8) [24]. Thus, unlike the use of the *N*-alkylated-PTA derivative as described before for the synthesis of the copper complexes **13**–**15**, in this synthetic procedure the *N*-alkylation of the phosphine occurred after the formation of the metal complex. As reported above for **13a** and **13b**, the heterogenized forms of **16** and **17** were obtained again by the immobilization of complexes on several carbon supports. In detail, the two tin complexes were anchored to activated carbon (**16**_AC and



Scheme 8. Synthetic procedure for the preparation of Sn complexes **16** and **17**.

Table 3

Catalytic cyanosilylation of benzaldehyde with carbon-supported tin complexes **16** and **17**^a.



Entry	Catalytic system	Time (min)	T (°C)	Isolated Yield ^b [%]
1	16 _AC	5	50	94.3
2	16 _AC-ox	5	50	12.0
3	16 _AC-ox-Na	5	50	26.6
4	16 _CNT	5	50	72.5
5	16 _CNT-ox	5	50	30.5
6	16 _CNT-ox-Na	5	50	27.8
7	17 _AC	5	50	85.9
8	17 _AC-ox	5	50	41.3
9	17 _AC-ox-Na	5	50	49.6
10	17 _CNT	5	50	82.7
11	17 _CNT-ox	5	50	29.7
12	17 _CNT-ox-Na	5	50	20.8
13	16 _AC	5	60	81.0
14	16 _AC	5	40	88.5
15	16 _AC	5	30	86.0
16	16 _AC	10	50	78.7
17	16 _AC	10	30	76.3
18	16 ^c	5	50	84.7

^a Reaction conditions: benzaldehyde (25 mmol), TMSCN (26 mmol), catalyst loading 0.1 mol% (based on the aldehyde).

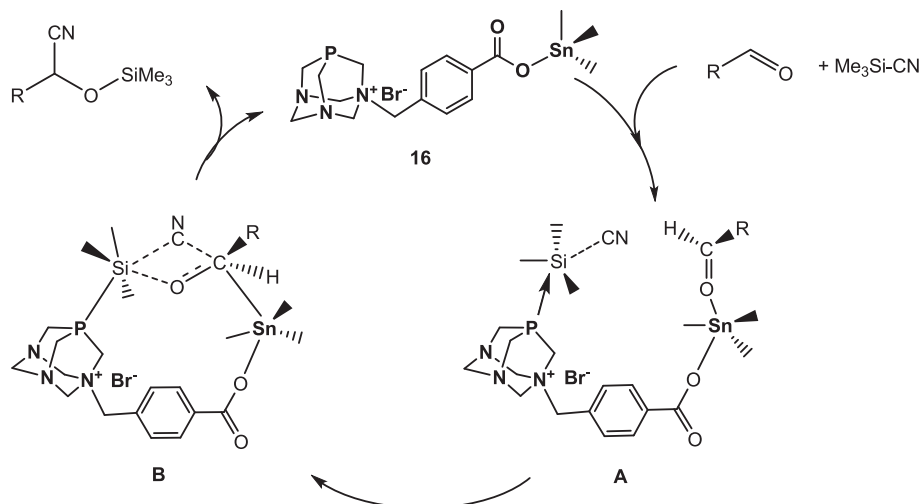
^b Determined by ¹H NMR.

^c Catalyst loading 1 mol%.

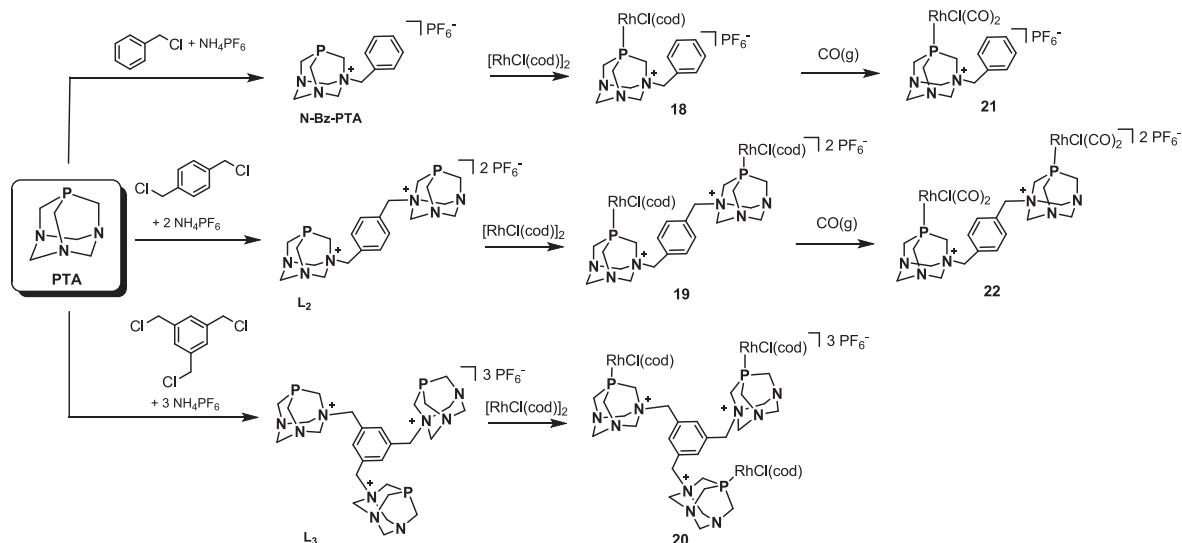
17_AC), to multi-walled carbon nanotubes (**16**_CNT and **17**_CNT) and to their corresponding oxidized forms obtained by treatment with HNO₃ (**16**_AC-ox, **17**_AC-ox, **16**_CNT-ox, **17**_CNT-ox), and treatment with NaOH (**16**_AC-ox-Na and **17**_AC-ox-Na; **16**_CNT-ox-Na and **17**_CNT-ox-Na).

The catalytic efficiency of all carbon-supported complexes was evaluated in aldehyde cyanosilylation reactions. In particular, the benzaldehyde and trimethylsilyl cyanide (TMSCN) was chosen as model substrates for the heterogeneous catalytic tests carried out at 50 °C under microwave irradiation (10 W), with 0.1 mol% catalyst loading and in solvent-free conditions (Table 3).

Both complexes **16** and **17** supported on AC and CNT resulted more active than their chemically treated counterparts, with the AC-supported materials showing a higher activity than complexes supported on CNT. Under these conditions, **16**_AC resulted the best catalytic system, yielding the cyanohydrin product in 94 %. The effects of temperature (30–60 °C) and time (5 or 10 min) on the system **16**_AC were also assessed, proving that the decrease of both parameters improved the catalytic performance (Table 3, entries 13–17). The activity of unsupported complex **16** was also investigated under standard conditions (50 °C, 10 W, 5 min). Catalyst **16** gave cyanohydrin in 85 % yield, a lower value compared to the 94 % yield obtained with the AC-supported version (Table 3, entries 18 and 1). Notably, also unsupported **16** resulted to be a heterogeneous catalyst, being insoluble in the reaction media. The catalytic system **16**_AC was also found to be a robust and recyclable heterogeneous catalyst in the cyanosilylation of benzaldehyde, still showing a yield of 72 % after the fourth cycle. This yield was increased up to 88 % when the catalyst was regenerated after each cycle by a chemical treatment to remove the reactants or other impurities adsorbed on the catalyst surface that blocked the active sites. Catalyst



Scheme 9. Proposed mechanism for aldehyde cyanosilylation using the double-activating supported catalyst **16** [24].



Scheme 10. Synthesis of *N*-benzylated PTA ligands and their corresponding Rh(I) complexes **18–22** [25a].

16_AC was tested further for the cyanosilylation of several aromatic and aliphatic aldehydes giving in most cases quantitative conversions after 5 min at 50 °C. A catalytic mechanism was proposed involving **16** as double-activating catalyst through the Sn(IV) and the uncoordinated phosphorus atom that act as Lewis acid and Lewis base, respectively (Scheme 9) [24].

3. Catalytic applications of precious metal-PTA complexes

Catalytic applications of precious metal complexes stabilized by PTA and derivatives reported in the period 2018–2024 focused essentially on the use of Rh and Ru, either as catalysts obtained *in situ* by mixing PTA and metal precursors, or as well-defined molecular complexes. Rh-PTA complexes found application in aqueous-biphasic hydroformylation of 1-octene, chemo- and regioselective hydroformylation of alkenes using CO₂/H₂ to replace syngas (CO/H₂), hydromethoxylation of alkenes to linear alcohols with CO₂/H₂, and acid-assisted hydrogenation of CO₂ to methanol. Ru-PTA complexes were applied for various catalytic processes, including allylic alcohol isomerization, formic acid and (acceptorless) alcohol dehydrogenation, alkyne and nitrile hydration. The main results are described in the following sections.

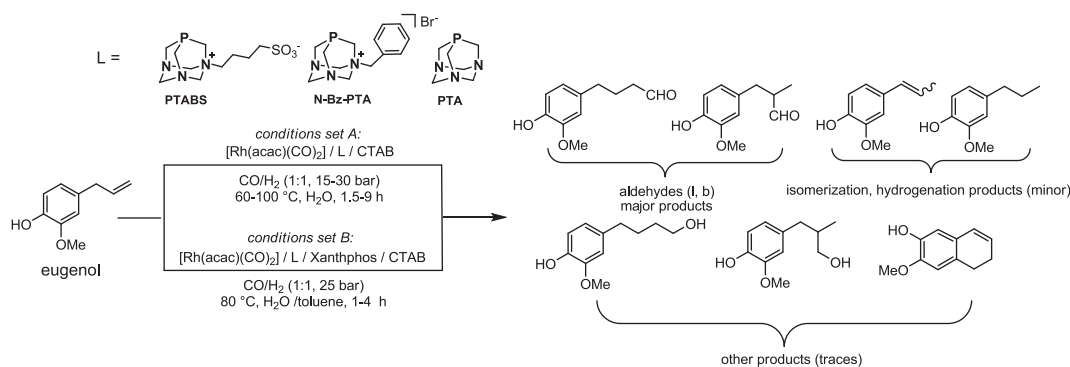
3.1. Rhodium

In 2018 Smith and coworkers described the synthesis of “lower-rim” PTA ligands, derived from *N*-quaternization of 1,4-bis(chloromethyl)benzene and 1,3,5-tris(chloromethyl)benzene with PTA and compared their coordination behavior to Rh(I) with that of cationic *N*-benzyl-PTA (*N*-Bz-PTA) [25a]. The syntheses of these mono- and bis-PTA derivatives had been previously reported by Kathó and coworkers [25b]. As expected, upon reaction of the ligands with [RhCl(cod)]₂ precursor [cod = η²-1,5-cyclooctadiene], the mono-, bi- and trimetallic complexes **18–20** were obtained. Complexes **18–19** were then converted to the corresponding bis-carbonyl derivatives **21–22** upon replacement of the η²-cod ligand by exposure to CO(g), as shown in Scheme 10.

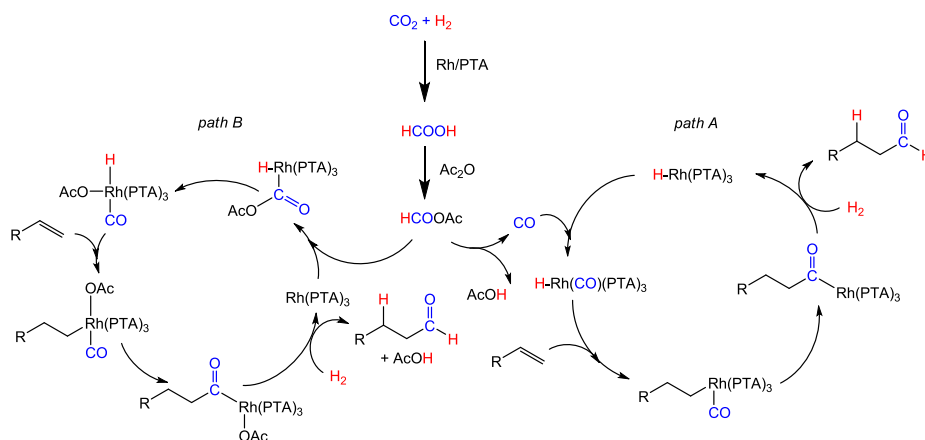
All complexes were tested for 1-octene hydroformylation in water/toluene (1:1) biphasic conditions, screening reaction parameters such as the type of catalyst, temperature, pressure and observing the effects on yields, chemo- and regioselectivity. In particular, the authors wanted to verify whether the presence of more than one metal center could induce cooperative interactions, enhancing the catalytic activity compared to the monometallic analogues. The experiments were performed at temperatures of 50, 75 and 95 °C and a syngas pressure (CO/H₂ = 1:1) of 20,

30 and 40 bars in toluene (5 mL) and water (5 mL) at a catalyst loading Rh:substrate = 1:2500. The highest conversions (>90 %) were obtained at 75 and 95 °C. Higher temperatures had an effect on regioselectivity, favoring branched aldehydes with **19** and **20**, whereas linear aldehydes were preferentially obtained at lower temperatures. No major effects were observed with **18**, as in both cases linear aldehydes were formed in higher ratios. Increasing the pressure had an impact on chemo-selectivity, favoring aldehyde formation over alkene isomerization/hydrogenation. In general, no significant effects on conversion and selectivity were observed passing from **18** to **19**, whereas reactions run at 50 °C gave higher conversions in the presence of **20**. The authors concluded that the major effect of increased nuclearity within the Rh (cod) complexes was rather on the reaction rate than on the overall conversion and selectivities. Under optimized conditions (75 °C, 40 bar), TOF values were observed in the range 200–292 h⁻¹, and the highest value was obtained using **18**. Bis(carbonyl) complexes **21** and **22** favored better regioselectivity toward linear aldehydes, with n:iso ratios up to 3.8 vs. values in the range 1.1–1.6 obtained with **18–20**. On the other hand, Rh(cod) complexes gave better chemoselectivity to aldehyde formation than the Rh-carbonyl analogues. Finally, recyclability tests were also performed, showing however a fast depletion of the catalyst from the aqueous layer, thus limiting practical applicability.

A very recent contribution by Bhanage and coworkers describes the use of another *N*-PTA “lower rim” derivative PTABS (KapdiPhos) as stabilizing ligand for biphasic and interface Rh-catalyzed eugenol hydroformylation, in the presence of CTAB (CTAB=cetyltrimethylammonium bromide) as phase-transfer agent [26]. The ligand was obtained by reaction of PTA with 1,4-butane sultone in acetone under reflux conditions (60 °C, 24 h). The initial goal of the study was to obtain a very active biphasic system giving high chemoselective aldehyde formation, minimizing the yield of hydrogenation and isomerization products, that could also allow for catalyst recycling by reuse of the water phase containing the catalyst. Reaction parameters screening identified the best conditions as: eugenol (1.64 g, 10 mmol), [Rh(acac)(CO)₂] (acac = acetylacetonate, 5.9 mg, 0.0225 mmol), PTABS (13.2 mg, 0.045 mmol), CTAB (3.3 mg, 0.009 mmol), distilled deionized degassed water (10 mL), 80 °C, CO/H₂ (1:1, 25 bar), 4 h. Under these conditions, full eugenol conversion was observed, with a maximum aldehyde yield of 93 % and linear to branched (l/b) ratio of 1.56. Ligand effects were also tested, comparing the results with those obtained using PTA or *N*-Bz-PTA instead of PTABS, but worse performances were observed, as in the case of use of different phase-transfer reagents (cyclodextrins in place of CTAB). Next, the authors tested the effect of



Scheme 11. Eugenol hydroformylation, reaction products and water-soluble PTA-type ligands [26].



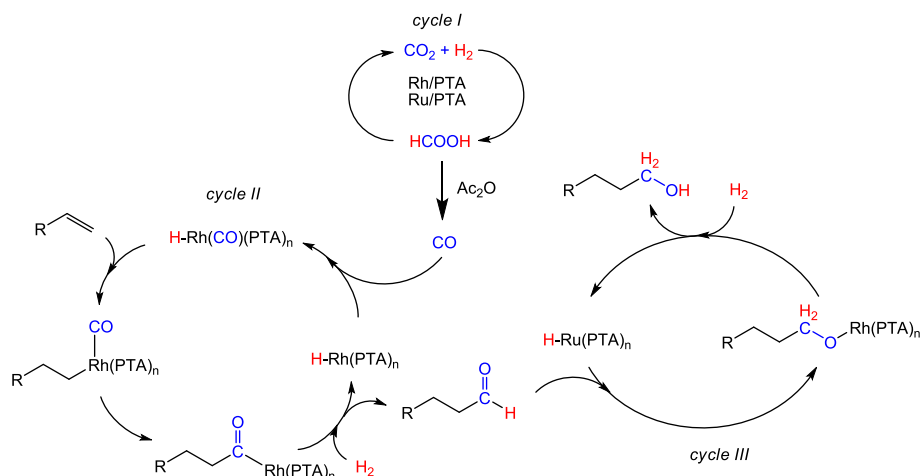
Scheme 12. Proposed interconnected mechanisms for alkene hydroformylation by CO_2/H_2 with Rh/PTA [27].

addition of the water-insoluble ligand 4,5-bis(diphenylphosphino)-9,9-dimethylxanthene (Xantphos) to the catalytic mixture, using toluene as organic solvent. Xantphos is one of the best-known ligands to favor high l/b ratios in olefin hydroformylation to aldehydes, and in this case the reaction would occur at the water-toluene interface. The reactions conditions were thus slightly modified as follows: eugenol (10 mmol), $[\text{Rh}(\text{acac})(\text{CO})_2]$ (0.0225 mmol), PTABS (0.135 mmol), CTAB (0.009 mmol), water (10 mL), Xantphos (13.0 mg, 0.0225 mmol), toluene (3.5 mL), CO/H_2 (1:1, 25 bar), 80 °C. At a Rh/PTABS/Xantphos ratio of 1:6:1, high yields in aldehydes (93 %) were obtained after 1.5 h, with a significant l/b ratio increase to 13.3. Catalyst recycling was demonstrated in up to four consecutive cycles, observing a gradual decrease in aldehyde yield, likely due to Rh leaching into the organic phase. The reaction scheme and the PTA-type ligands are shown in Scheme 11.

An interesting application of Rh/PTA-based catalytic protocols was disclosed in 2021 by Liu, Wang, Sun and coworkers [27]. In the quest for new strategies for chemo- and regioselective hydroformylation of alkenes using CO_2/H_2 as a syngas surrogate, the authors tested the combination of $[\text{Rh}(\text{acac})(\text{CO})_2]$ with various mono- and bidentate ligands to make *in situ* catalysts able to promote tandem CO_2 hydrogenation to HCOOH , followed by formation of HCOOAc in the presence of acetic anhydride (Ac_2O), that in turn releases $\text{CH}_3\text{CO}_2\text{H}$ and CO , with the latter then available for conventional hydroformylation reaction. The study started testing 1-decene as a substrate, under 25 bar CO_2/H_2 (4:1) in the presence of Ac_2O , $[\text{Rh}(\text{acac})(\text{CO})_2]$ and ligands such as PPh_3 , TPPTS, Xantphos, BISBI, dppf, dppb, PTA [TPPTS=tris(3-sulfophenyl)phosphine trisodium salt; BISBI=2,2'-Bis(diphenylphosphinomethyl)-1,1'-biphenyl; dppf = 1,1'-bis(diphenylphosphino)ferrocene; dppb = 1,2-bis(diphenylphosphino)butane] in NMP (NMP=*N*-methylpyrrolidone) as solvent, 80 °C, 12 h. It was shown that the Rh/dppb system could promote hydroformylation to aldehydes (87 % yield) with l/b ratio = 78:22.

An even better regioselectivity was obtained replacing dppb with PTA (l/b = 89/11). Substrate scope was then explored in the presence of Rh/PTA=1:6, testing numerous terminal alkenes (C5–C10), obtaining similar reactivity irrespective of the carbon chain length, obtaining aldehydes in over 90 % yields with good linear regioselectivities (l/b = 85:15–90:10). The key of the success of PTA resides in the fast production of HCOOAc or CO , in turn stemming from the high activity of this system to generate HCOOH through CO_2 hydrogenation in acidic media. By a combination of isotope labelling and control experiments, the authors were able to propose two interconnected catalytic cycles that could equally contribute to the overall mechanism (Scheme 12). In path A, CO_2 is hydrogenated by Rh/PTA to HCOOH , which dehydrates to CO in the presence of Ac_2O . Next, Rh/PTA-catalyzed conventional hydroformylation proceeds smoothly in the presence of H_2 and *in situ* generated CO . In unconventional path B, *in situ* formed HCOOAc acts as a direct carbon source, and Rh-acetate species are involved. The authors proposed that this pathway is most active in the early stage of the reaction, and favors linear aldehydes formation.

In the same year, the same authors expanded on this concept and demonstrated the feasibility of selective production of linear alcohols by hydroxymethoxylation reactions from alkenes and CO_2/H_2 through a bimetallic Rh – Ru catalyst using PTA as the ligand, in up to 92 % yield with 87/13 regioselectivity [28]. The catalytic protocol involved the presence of an alkene (initially 1-octene, 1 mmol), $\text{Rh}(\text{acac})(\text{CO})_2$ (0.02 mmol), PTA (0.12 mmol), $\text{Ru}(\text{acac})_3$ (0.02 mmol), Ac_2O (2.0 mmol), $\text{CO}_2/\text{H}_2 = 20/5$ bar, NMP (4 mL). The test were carried out with two distinct temperature ramps T_1 and T_2 , in order to favor hydroformylation and hydrogenation conditions, respectively. The most efficient temperature and time intervals proved to be $T_1 = 100$ °C, $t_1 = 12$ h, $T_2 = 120$ °C, $t_2 = 12$ h. The tandem process gave excellent alcohol yield (89 %) and regioselectivity (l/b = 85:15). Substrate scope included 8



Scheme 13. Proposed domino cascade reactions for alkene hydroxymethylation by CO_2/H_2 with Rh-Ru/PTA [28].

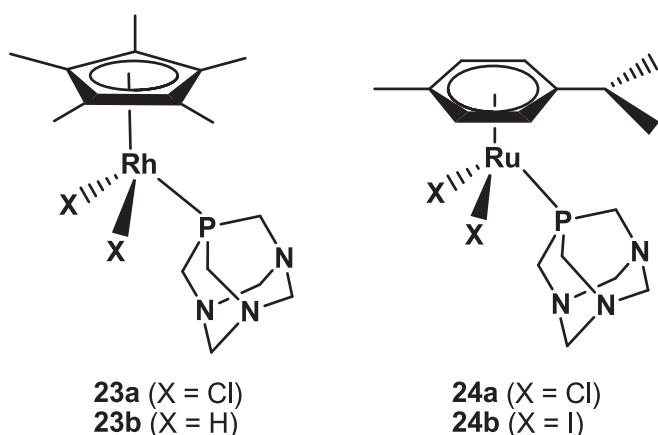


Fig. 6. Molecular drawings of complexes **23** and **24** [29].

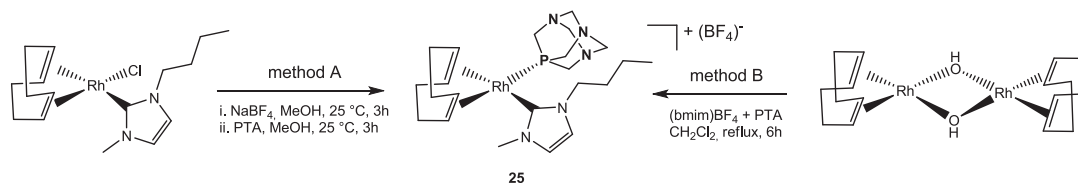
different terminal alkenes, and internal alkenes such as cycloalkenes, norbornene and 2-octene, reaching good results in terms of alcohol yields and regioselectivities (64 – 92 %, 1/b = 80:20 – 91:9). Interestingly, control experiments showed that the role of Ru/PTA was both to catalyze the hydrogenation of aldehydes and to inhibit the hydrogenation and isomerization of alkenes. A domino sequence of three catalytic cycle was then proposed to account for the reaction mechanism (Scheme 13). Initially, CO_2 is hydrogenated by Rh/PTA and Ru/PTA to produce HCOOH (cycle I), which decomposes to $\text{CO} + \text{H}_2\text{O}$, assisted by Ac_2O . In the presence of H_2 and *in situ* generated HCOOH or CO , Rh/PTA-catalyzed hydroformylation gives preferentially linear aldehydes (cycle II). Notably, during the hydroformylation process, Ru/PTA inhibits the hydrogenation and isomerization of alkenes promoting instead CO_2 hydrogenation. The aldehyde is finally hydrogenated by Ru/PTA to produce the desired linear alcohol product (cycle III).

A highly desired chemical transformation is the conversion of CO_2 to CH_3OH by catalytic hydrogenation. In 2021, Trivedi, Kumar, Rath and coworkers published results on the use of Rh(III) cyclopentadienyl and

Ru(II) arene (also known as RAPTA-type) complexes bearing PTA (Fig. 6) as efficient catalysts for this process [29a].

In the case of Rh, complex $[\text{Cp}^*\text{RhCl}_2(\text{PTA})]$ (**23a**) was synthesized from the reaction of $[\text{Cp}^*\text{RhCl}_2]_2$ with PTA [29b]. Reaction of **23a** with NaBH_4 (xs) gave the *N*- BH_3 -PTA intermediate $[\text{Cp}^*\text{Rh}(\text{H})_2(\text{PTA}-\text{N}-\text{BH}_3)]$, that was then hydrolyzed at 60°C to give $[\text{Cp}^*\text{Rh}(\text{H})_2(\text{PTA})]$ (**23b**) [29c]. Similarly, complexes $[\text{RuCl}_2(p\text{-cymene})(\text{PTA})]$ (**24a**) and $[\text{RuI}_2(p\text{-cymene})(\text{PTA})]$ (**24b**) were obtained from the reaction of the corresponding Ru-arene dimers with PTA [29d]. At first, the authors tested the complexes for the hydrogenation of ethyl and methyl formate, that occurred efficiently at 60°C , 24 h, 1 bar H_2 , in the presence of MSA (MSA = methanesulfonic acid), with TONs in the range 930–1920 using **24b**. Next, the direct hydrogenation of CO_2 to CH_3OH was carried out, under the conditions: catalyst (0.0025 mmol), $\text{CH}_3\text{CH}_2\text{OH}$ (10 mmol), THF (5 mL), H_2 (3 atm), CO_2 (1 atm), MSA (1 mL), 60°C , 24 h. In the case of Rh complex **23b**, a yield of 28 % (TON=1120) was obtained. Under the same conditions, the Ru complexes **24a** and **24b** gave better performances, with yields of 36 % (TON=1440) and 49 % (TON=1944), respectively. Further screening of the influence of catalyst loadings, additive and reaction time was carried out using in particular **24b**. It was showed that, by replacing MSA with HNTf_2 (HNTf_2 = bis-(trifluoromethane)sulfonamide) and increasing the reaction times from 8 to 72 h, TON increased by an order of magnitude (from 300 to 3090). In general, Rh complexes showed lower activities than the Ru counterparts. In details, for Rh the highest TON=1680 was obtained with **23b** and HNTf_2 (1.0 equiv.) after 24 h, whereas under the same conditions a TON of 4752 (yield = 95 %) was observed in the presence of **24b**. Mechanistic details highlighted the role of metal-coordinated PTA as proton shuttle, mediating the formation of the active metal-hydrido species, thanks to the presence of highly basic N atoms at the cage bottom.

New water-soluble *N*-heterocyclic carbene (NHC) or mixed NHC/tertiary phosphine complexes $[\text{RhCl}(\text{cod})(\text{sSImes})]$, $\text{Na}_2[\text{Rh}(\text{bmim})(\text{cod})(\text{TPPMS})]$ and $[\text{Rh}(\text{bmim})(\text{cod})(\text{PTA})]\text{BF}_4$ (**25**) were described by Czégényi and coworkers in 2020 and applied as catalysts in redox isomerization of allylic alcohols to the corresponding ketones in aqueous media [sSImes = 1,3-bis(2,4,6-trimethyl-3-sodiumsulfonatophenyl)



Scheme 14. Synthesis of $[\text{Rh}(\text{bmim})(\text{cod})(\text{PTA})]\text{BF}_4$ (**25**) [30].

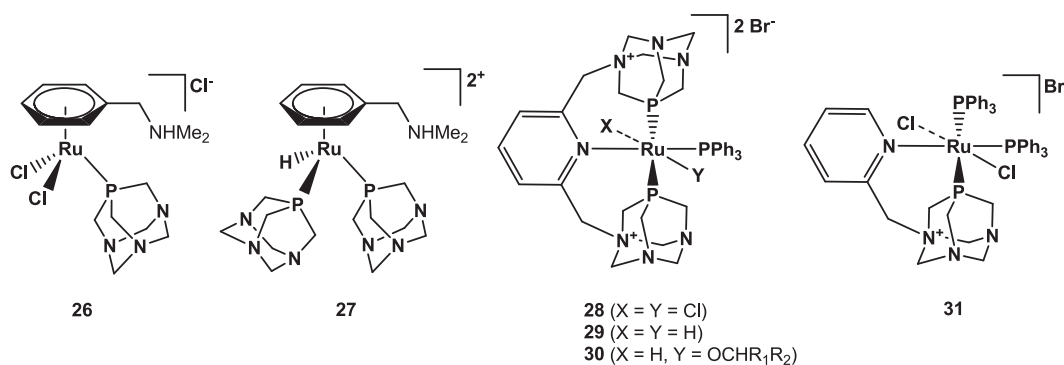


Fig. 7. Molecular drawings of complexes 26–31 involved in dehydrogenation reactions [31–34].

imidazolin-2-ylidene; bmim = 1-butyl-3-methyl-imidazol-2-ylidene, TPPMS=mono(3-sulphophenyl)phosphine sodium salt [30]. Complex 25 was obtained using two different synthetic pathways, namely by method (A), *i.e.* reacting $[\text{Rh}(\text{OH})(\text{cod})]_2$ with 1-butyl-3-methylimidazolium-tetrafluoroborate ($[\text{bmimH}]\text{BF}_4$) and PTA under reflux condition and method (B), by chloride removal from $[\text{RhCl}(\text{bmim})(\text{cod})]$ with NaBF_4 in MeOH at room temperature, followed by addition of 1 equiv. of PTA to the solution (Scheme 14).

Complex 25 was tested as catalyst for allylic alcohol isomerization for a small library of substrates, differing for the length of the alkyl chain, from *n*-propyl to *n*-octyl. Using a substrate to catalyst ratio of 1000:1, neat water, 80 °C, 30 min, buffered pH=7.0, conversions in the range 15–94 % were observed, with the highest obtained for pent-1-en-3-ol and corresponding to TOF=67 h⁻¹. Under the same reaction conditions, the catalyst obtained *in situ* by mixing $[\text{RhCl}(\text{cod})(\text{sSImes})]$ with TPPMS (1 equiv.) gave however better overall performances, with conversions in the range 44–73 % and TOFs in the range 88–152 h⁻¹.

3.2. Ruthenium

In the period 2018–2024, reports on formic acid and (acceptorless) alcohol dehydrogenation, allylic alcohol isomerization, alkyne and nitrile hydration reactions catalyzed by Ru-PTA and Ru-PTA derivative complexes were disclosed, together with studies on mechanistic details of some of these reactions. Some of these data have already been summarized in a previous review article dedicated to Ru(II)-phosphaurotropine complexes and catalysis [9].

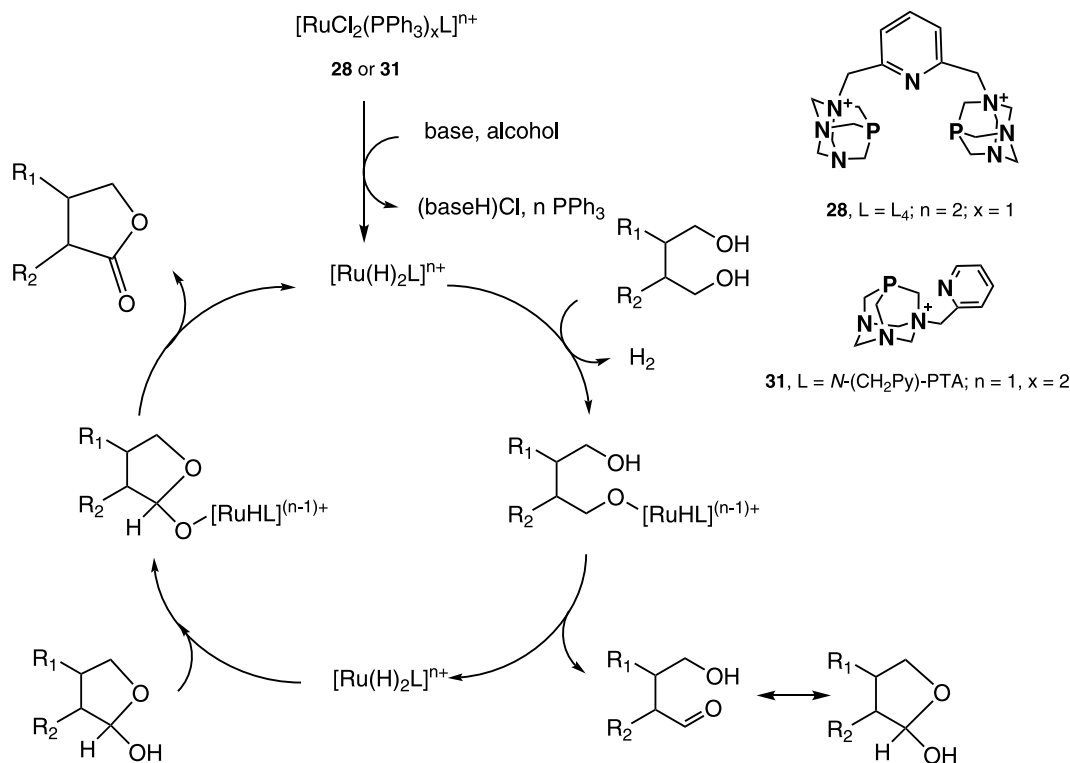
The catalytic dehydrogenation of hydrogen-rich organic carrier molecules is a protocol of interest in the search of methods to exploit chemical bond reactivity for the production and storage of hydrogen. Among the families of organic compounds from which hydrogen can be extracted, the most studied are simple carboxylic acids and alcohols. For the first class, formic acid (HCOOH) has received a greater attention. In 2018, Fink, Laurency and coworkers expanded on the body of results previously published with similar systems, disclosing mechanistic studies on the role of a RAPTA-type complex, $[(\eta^6\text{-benzylidimethylamine})\text{RuCl}_2(\text{PTA})]\text{Cl}$ (26), as recyclable catalyst for the selective water-phase HCOOH dehydrogenation to H₂ + CO₂ gas mixture [31]. The complex (Fig. 7) was synthesized from dimeric $[(\eta^6\text{-benzylidimethylamine})\text{RuCl}_2]_2\text{Cl}_2$ precursor and one equivalent of PTA per central Ru atom. The piano-stool type catalyst presents a η^6 -arene with a dimethylamino group attached to the ring by a single methylene spacer, to prevent this moiety from interacting with the central Ru atom by its lone pair. Amino groups can be beneficial in water-phase catalysis, *i.e.* by acting as proton shuttle centers, by increasing catalysts water solubility, and by participating in substrate activation mechanism favoring hydrogen bonding with the water media. The catalytic tests were run in closed vessels at 70–100 °C in the presence of HCOOH (222 mg) dissolved in 1778 mg of water, at a catalyst loading of 0.0165 M. At all temperatures, full conversion was observed, with different kinetics.

Under these conditions, catalyst recyclability was not possible, due to Ru metal deposition indicative of catalyst decomposition. The addition of free PTA to the reaction mixture increased catalyst stability and recyclability. By comparison of the energies of activation E_a derived from the corresponding Arrhenius plots, a lower value ($88.67 \pm 4 \text{ kJ mol}^{-1}$) was measured in the presence of added PTA, compared to the system without this addition ($95.59 \pm 4 \text{ kJ mol}^{-1}$). For the latter system, *in situ* NMR monitoring allowed to identify signals that were attributed to the active monohydrido species $[(\eta^6\text{-benzylidimethylamine})\text{RuH}(\text{PTA})_2]^{2+}$ (27), shown in Fig. 7.

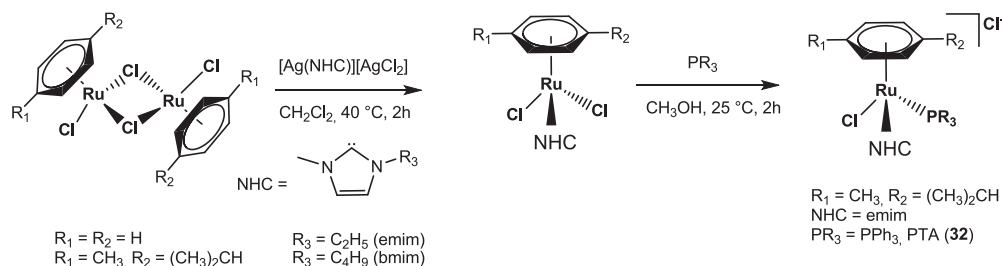
In 2018, Bhatia and Muthaiah described the use of the pincer-type complex $[\text{RuCl}_2(\text{PPh}_3)(\text{L}_4)]\text{Br}_2$ (25, Fig. 7) as well-defined molecular catalyst for acceptorless alcohol dehydrogenation (AAD) reactions [32]. The tridentate PNP ligand L₄ (Fig. 1) was obtained by reaction of 2,6-bis(bromomethyl)pyridine with 2 equiv. of PTA, then the corresponding complex 28 was synthesized by reaction of the ligand with 1 equiv. of $[\text{RuCl}_2(\text{PPh}_3)_3]$ precursor. The authors tested 28 (5 mol%) at first for the acceptorless dehydrogenation of 1-phenylethanol (0.5 mmol) to acetophenone, in the presence of a base (15 mol %) in refluxing H₂O (0.6 mL) for 24–48 h. Under optimized conditions, KO^tBu as base, 48 h, a maximum 91 % yield in product was achieved. Substrate scope was then explored including substituted aromatic secondary alcohols, cyclic and linear aliphatic alcohols, obtaining yields in the range 35–92 %. NMR mechanistic studies on stoichiometric reactions suggested that pre-catalyst 28 converts in the presence of base into the bis(hydrido) derivative $[\text{Ru}(\text{H})_2(\text{PPh}_3)(\text{L}_4)]\text{Br}_2$ (29). Complex 29 then activates the secondary alcohol substrate R₁R₂CHOH to give the alkoxy-species $[\text{RuH}(\text{OCHR}_1\text{R}_2)(\text{PPh}_3)(\text{L}_4)]\text{Br}_2$ (30) and free H₂. In the final step, ketone is released to regenerate 29, closing the catalytic cycle.

The same authors studied the application of the related Ru complex $[\text{RuCl}_2(\text{PPh}_3)_2\{N\text{-(CH}_2\text{Py)PTA}\}]\text{Br}$ [31, Fig. 7; N-(CH₂Py)-PTA = {1-N-(pyridin-2'-yl-methyl)-1,3,5-triaza-7-phosphaadamantyl}bromide, Fig. 1] as catalysts for the same type of reaction in aqueous media [33]. The complex was synthesized by reaction of $[\text{RuCl}_2(\text{PPh}_3)_3]$ with the ligand under reflux conditions in toluene for 12 h. The molecular formula of 31 was proposed based on ¹H, ³¹P{¹H}, ¹³C{¹H} NMR spectroscopy data and mass analysis, but was not drawn in the original publication. Reaction conditions were optimized based on 1-phenylethanol oxidation to acetophenone, for which a maximum yield of 93 % was obtained using substrate (0.5 mmol), KOH (15 mol%), catalyst (5 mol %), H₂O (0.6 mL), 100 °C, 48 h. Next, the optimized protocol was applied to variously substituted aryl and alkyl secondary alcohols, with yields in the range 43–94 %. Primary alcohols such as phenylmethanol and *p*-methoxyphenylmethanol were also tested as substrates, showing moderated yields (36 and 38 %, respectively) to the corresponding aldehydes. Mechanistic studies suggested that the active species in catalysis is obtained by loss of two PPh₃ ligands from 31, followed by the typical Bäckvall-type oxidation mechanism.

Next, the same research group disclosed results on the use of 28 and 31 as catalysts for acceptorless lactone synthesis from diols in water



Scheme 15. Proposed mechanism for 1,4-butanediol lactonization catalyzed by **28** and **31** [34].



Scheme 16. Synthesis of $[\text{RuCl}_2(\text{NHC})(\eta^6\text{-arene})]$ and $[\text{RuCl}(\text{NHC})(\eta^6\text{-arene})(\text{PR}_3)]\text{Cl}$ complexes [35].

[34]. Under the abovementioned conditions used in the previous work, 1,4-butanediol was successfully converted into butyrolactone with yields up to 57 % and 48 % with **28** and **31**, respectively. By increasing the catalyst loading to 10 mol%, and varying KOH amount in the range 20–30 mol%, yields as high as 95 % were obtained with **31**. The optimized catalytic protocol was then applied to a series of alkyl and aryl diols, obtaining four-, five- and six-membered ring lactones in high yields (up to 97 %). In general, better results were obtained with **31** as catalyst, probably due to ligand hemilability that may help substrate coordination to the metal center. Based on NMR experiments with 1,4-butanediol as substrate, the authors proposed an inner-sphere catalytic mechanism based on Ru-dihydrido species, shown in **Scheme 15**.

Related to hydrogenation/dehydrogenation processes, the catalytic racemization of optically active secondary alcohols is a process of interest for research, in particular in the field of dynamic kinetic resolution. In 2018, Marozsán, Joó and coworkers reported the synthesis of novel Ru(arene)(NHC)-type complexes (NHC = *N*-heterocyclic carbene) and their use as catalysts for this process [35]. In detail, five new complexes of the type $[\text{RuCl}_2(\text{NHC})(\eta^6\text{-arene})]$ and $[\text{RuCl}(\text{NHC})(\eta^6\text{-arene})(\text{PR}_3)]\text{Cl}$ [NHC = 1-butyl-3-methylimidazolium (bmim), 1-ethyl-3-methylimidazolium (emim); arene = benzene, *p*-cymene; PR_3 = PPh_3 , PTA) were synthesized and applied as catalysts for chiral secondary alcohol racemization, comparing the results with those obtained with

$[\text{RuCl}_2(\text{bmim})(\eta^6\text{-}p\text{-cymene})]$, with and without added free PPh_3 . The general synthetic pathway to the complexes is depicted in **Scheme 16**. The appropriate Ru(arene) dimer precursors were reacted with $[\text{Ag}(\text{NHC})][\text{AgCl}_2]$ salts to obtain the corresponding $[\text{RuCl}_2(\text{NHC})(\eta^6\text{-arene})]$ derivatives. $[\text{RuCl}_2(\text{emim})(\eta^6\text{-}p\text{-cymene})]$ was further reacted with PPh_3 or PTA to obtain the corresponding $[\text{RuCl}(\text{emim})(\eta^6\text{-}p\text{-cymene})(\text{PR}_3)]\text{Cl}$ (**32**, PR_3 = PTA).

The authors tested the racemization of (*S*)-1-phenylethanol (0.252 M) in toluene at 95 °C for 4 h, with a catalyst concentration of 0.01 M. In the case of added free ligand, a concentration of 0.01 M was also used (1:1 to metal). The best results were obtained using $[\text{RuCl}_2(\text{bmim})(\eta^6\text{-}p\text{-cymene})] + \text{PPh}_3$, giving a residual enantiomeric excess (*ee*) as low as 1.3 %. It was observed however that, also for the best performing catalytic system, unwanted oxidation to acetophenone occurred as side reaction, up to 20.4 %. It was possible to minimize the quantity of acetophenone to 3.5 %, still reaching high levels of racemization (residual *ee* = 3.4 %) by changing the solvent to toluene/isopropanol = 5:1 mixture. Other chiral secondary alcohols were also tested, with less efficient results. Complex **32** showed modest activity, with residual *ee* = 20.5 %, and acetophenone yield = 4.8 %. Theoretical mechanistic studies by density functional theory (DFT) calculations starting from $[\text{RuCl}_2(\text{emim})(\eta^6\text{-}p\text{-cymene})(\text{PPh}_3)]$ suggested that the active species $[\text{Ru}(\text{emim})(\eta^6\text{-}p\text{-cymene})]^{2+}$ is formed from the parent complex upon

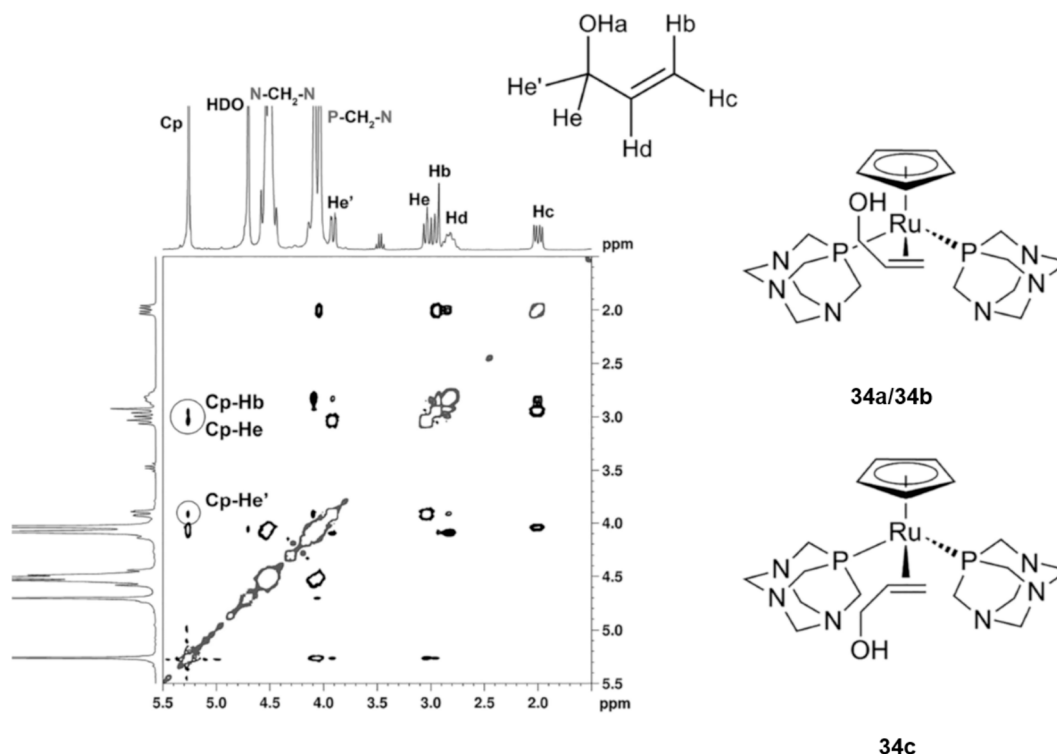


Fig. 8. ^1H - ^1H NOESY spectrum of **34a-c** in D_2O . Reprinted with permission from [37], copyright 2018 American Chemical Society.

loss of coordinated chloride and PPh_3 mainly due to steric congestion around the metal center.

Allylic alcohols catalytic isomerization in water has been widely studied, showing the importance of Ru-PTA complexes as catalysts for this kind of reactions [36]. In the period 2018–2024, further studies were published, addressing both mechanistic details and catalytic applications.

Romerosa and coworkers expanded further on their previous studies in this area and in 2018 disclosed results on the study of water participation by atomistic approach to solvent effects [37]. Previously, they showed that the activity of complex $[\text{CpRu}(\text{H}_2\text{O}-\kappa\text{O})(\text{PTA})_2](\text{CF}_3\text{SO}_3)$ (**33**) in the isomerization of allylic alcohols is strongly dependent on the choice of reaction medium. Experimentally, it was observed that the catalytic isomerization of 1-propen-3-ol, albeit modest, was higher when water was used as solvent instead of CH_3OH or $(\text{CH}_3)_2\text{CHOH}$. The authors applied a combination of NMR measurements, *ab initio* molecular dynamics (AIMD) simulations, neutron scattering experiments and empirical potential structure refinement (EPSR) simulations to identify the effect of water on the stability and reactivity of different conformational isomers derived from the interaction of **33** with a model allylic alcohol such as 1-propen-3-ol. The stoichiometric reaction of **33** with 1-propen-3-ol was carried out, with formation of the stable water-soluble η^2 -allylic complex $[\text{CpRu}(\text{exo-}\eta^2\text{-CH}_2=\text{CH}-\text{CH}_2-\text{OH})(\text{PTA})_2]^+$ (**34**), identified by ^1H - ^1H NOESY NMR experiment as two conformers (**34a,b**) shown in Fig. 8. The formation of the *endo*-isomer (**34c**) was less probable, due to steric hindrance.

Next, four different conformational isomers of **34** were modeled by density functional theory (DFT): the two η^2 -exoallyl isomers **34a** and **34b** differing for the increased dihedral angle of the alkyl C–C bond in **34b** that causes the allylic hydroxyl group to face away from the complex, the η^2 -endoallyl isomer **34c** and the O-coordinated isomer **34d**. *Ab Initio* Molecular Dynamics (AIMD) simulations based on these structures showed that, by increasing the number of H_2O molecules surrounding the complexes, these align to form a three-membered water chain between the hydrogen atom of the allylic-hydroxyl group (H_a) and one of the nitrogen atoms of a PTA ligand. The hydrogen-bonding chain is

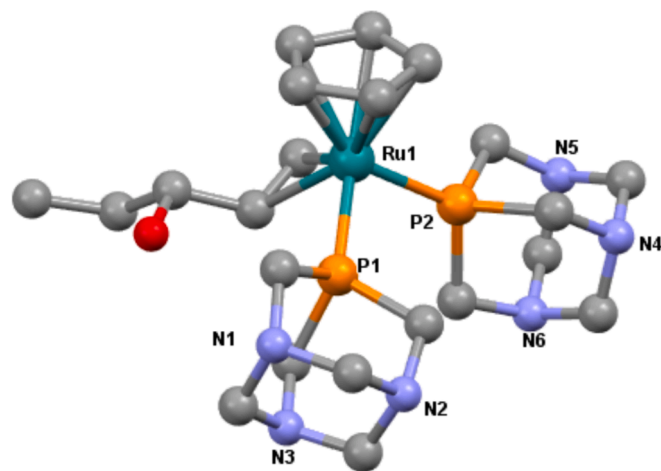
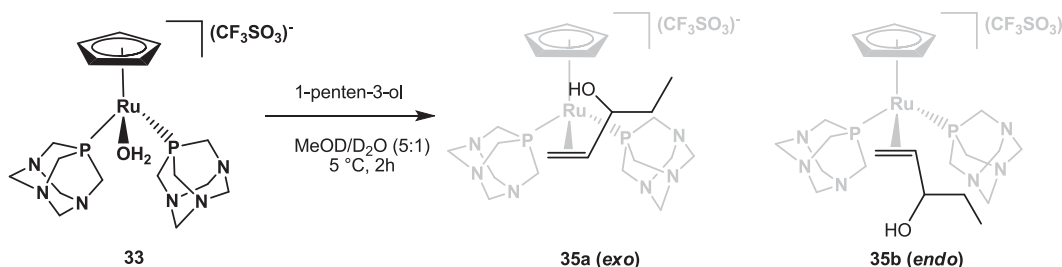


Fig. 9. X-ray crystal structure of **35a**. Hydrogen atoms, H_2O molecules and anion omitted for clarity. Drawing by CCDC Mercury® 3.9 [38].

favorable for **34a** over **34b**, forming faster and being more stable even at higher simulated temperature, whereas it has only transient behavior with **34c**. These results were also supported by neutron scattering experiments, and substantiate the hypothesis that water molecules can interact differently and stabilize specific conformers derived from the coordination of the substrate to the metal center.

Two years later, the same authors studied mechanistic details of the water-phase isomerization of 1-penten-3-ol in the presence of **33**, that was previously shown to occur fastly at 55°C when the water content was higher than 50 equivalents [38]. Reaction of **33** with 1-penten-3-ol in water/EtOH (1:10) afforded single crystals of $[\text{CpRu}(\text{PTA})_2(\text{exo-}\eta^2\text{-CH}_2=\text{CHOHCH}_2\text{CH}_3)](\text{CF}_3\text{SO}_3)\cdot 2\text{H}_2\text{O}$ (**35a**), allowing for the first X-ray crystal structure determination of a Ru(η^2 -allylic alcohol) complex (Fig. 9), featuring an extended network of weak hydrogen bonding, with distances larger than 2.5 \AA . The structure shows a typical piano-stool



Scheme 17. Formation of 35a and 35b from 33 [38].

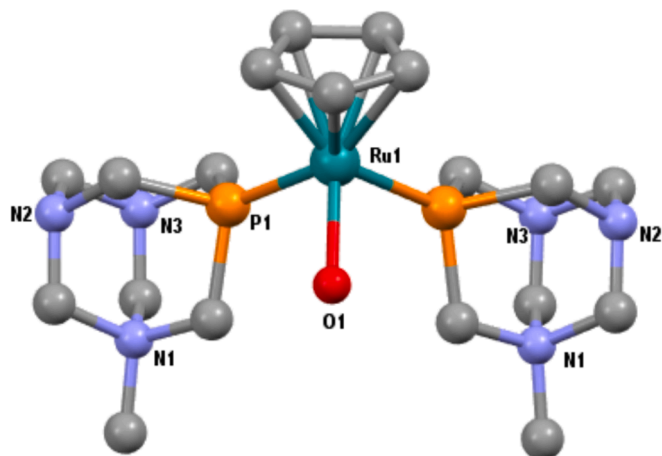


Fig. 10. X-ray crystal structure of 37. Hydrogen atoms, solvent molecules and anions omitted for clarity. Drawing by CCDC Mercury® 3.9 [39].

geometry, made of a η^5 -coordinated cyclopentadienyl ring, two P-coordinated PTA ligands and the η^2 -bound allylic alcohol moiety. The isomerization reaction was monitored by NMR spectroscopy. At 273 K in $\text{CD}_3\text{OD}/\text{D}_2\text{O}$ (5:1), $^{31}\text{P}\{^1\text{H}\}$ NMR showed two new AB systems in a 5.4:1 ratio, corresponding to the two different isomers 35a and 35b (Scheme 17), that were further studied by $^1\text{H}-^1\text{H}$ COSY and 1D-TOCSY NMR techniques. Interestingly, Eyring analysis showed that the *exo-endo* interconversion is strongly influenced by the presence and amount of water in solution, suggesting the existence of aggregating and disrupting hydrogen bonding networks. In detail, it was demonstrated that in the *exo-endo* equilibrium, the rate of the forward reaction is faster than that of the reverse one at temperatures above 289.8 K and that this could be correlated to the catalytic efficiency, favored in 35b for steric and electronic reasons.

In the following study, the authors tested complexes $[\text{CpRuCl}(\text{mPTA})_2](\text{CF}_3\text{SO}_3)_2$ (36) and $[\text{CpRu}(\text{H}_2\text{O}-\kappa\text{O})(\text{mPTA})_2](\text{CF}_3\text{SO}_3)_3$ (37) for the catalytic isomerization of the cyclic allylic alcohol 2-cyclohexen-1-ol to cyclohexanone (mPTA=*N*-methyl-1,3,5-triaza-7-

phosphaadamantane) [39]. For complex 37, single crystal X-ray structure determination was also obtained, showing a piano-stool geometry around the Ru center with a η^5 -coordinated cyclopentadienyl ring, two P-coordinated mPTA ligands, with the methyl groups pointing away from the Cp ring for steric reasons, and a κ^1 -O water molecule (Fig. 10). The rationale behind the use of 36 and 37, whose molecular structures are shown in Fig. 11, was that the PTA counterparts, although active for this reaction, showed poor catalyst recyclability under biphasic conditions and major loss of activity in subsequent runs due to depletion of the active species 33 from the water phase. Thus, the increased water solubility of the mPTA complexes should prevent this effect. In the presence of 1 mol% of catalyst, complex 37 generally performed better than 36, reaching a maximum TON=95 (yield = 95 %) after 5 h, 80 °C, N_2 atmosphere, $\text{CH}_3\text{OH}/\text{H}_2\text{O}$ (1:1) solvent mixture. Catalyst recycling experiments in cyclohexane/water (1:1, pH=1.7), 80 °C, 7 h, N_2 atmosphere gave an overall TON=471 after 7 consecutive runs. Interestingly, it was shown that the process could be also run without the need of N_2 atmosphere (*i.e.* under air), with a slight decrease of activity (overall TON, 5 runs: 382). In spite of these promising results, a gradual loss of activity was observed during catalyst recycling for both experimental setups. Mechanistic studies by NMR techniques in $\text{CD}_3\text{OD}/\text{D}_2\text{O}$ showed the formation of an η^2 -allyl alcohol intermediate, similar to what was previously observed for the isomerization of 1-penten-3-ol in the presence of 33.

After this study, the authors re-examined the application of 33 and its chloride analogue $[\text{CpRuCl}(\text{PTA})_2]$ (38, Fig. 11, right) for the catalytic isomerization of a substituted cyclic allylic alcohol, namely 3-methyl-2-cyclohexen-1-ol, a naturally occurring aggregative pheromone of the Douglas-fir beetle, a pest of coniferous trees [40].

Interestingly, results showed that, besides the desired isomerization of 3-methyl-2-cyclohexen-1-ol into 3-methylcyclohexanone (A), side reactions such as the oxidation into 3-methyl-2-cyclohexenone (B) and 1,3-transposition to 1-methyl-2-cyclohexen-1-ol (C), could be triggered under appropriate reaction conditions. Initially, complex 38 (10 mol%) was tested in water at 70 °C, under air for 24 h. Under these conditions, the product distribution (% yields) was determined as A:B:C=14:34:4, and at 72 h the yield of the oxidation product C raised to 55 %. By decreasing the amount of catalyst to 1 mol%, after 5 h under N_2 atmosphere, a ratio A:B=36:33 was obtained, whereas under air, oxidation

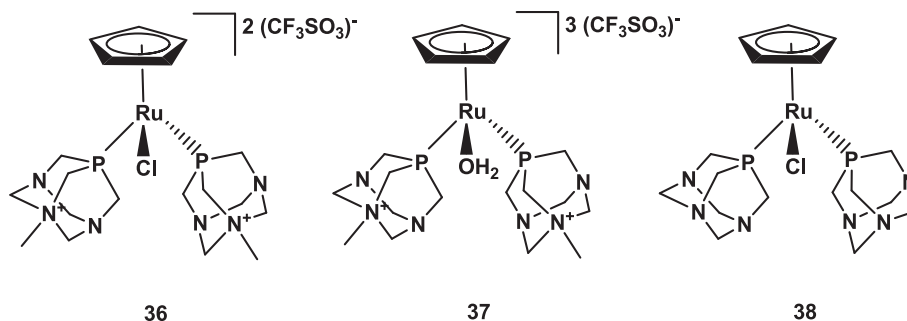
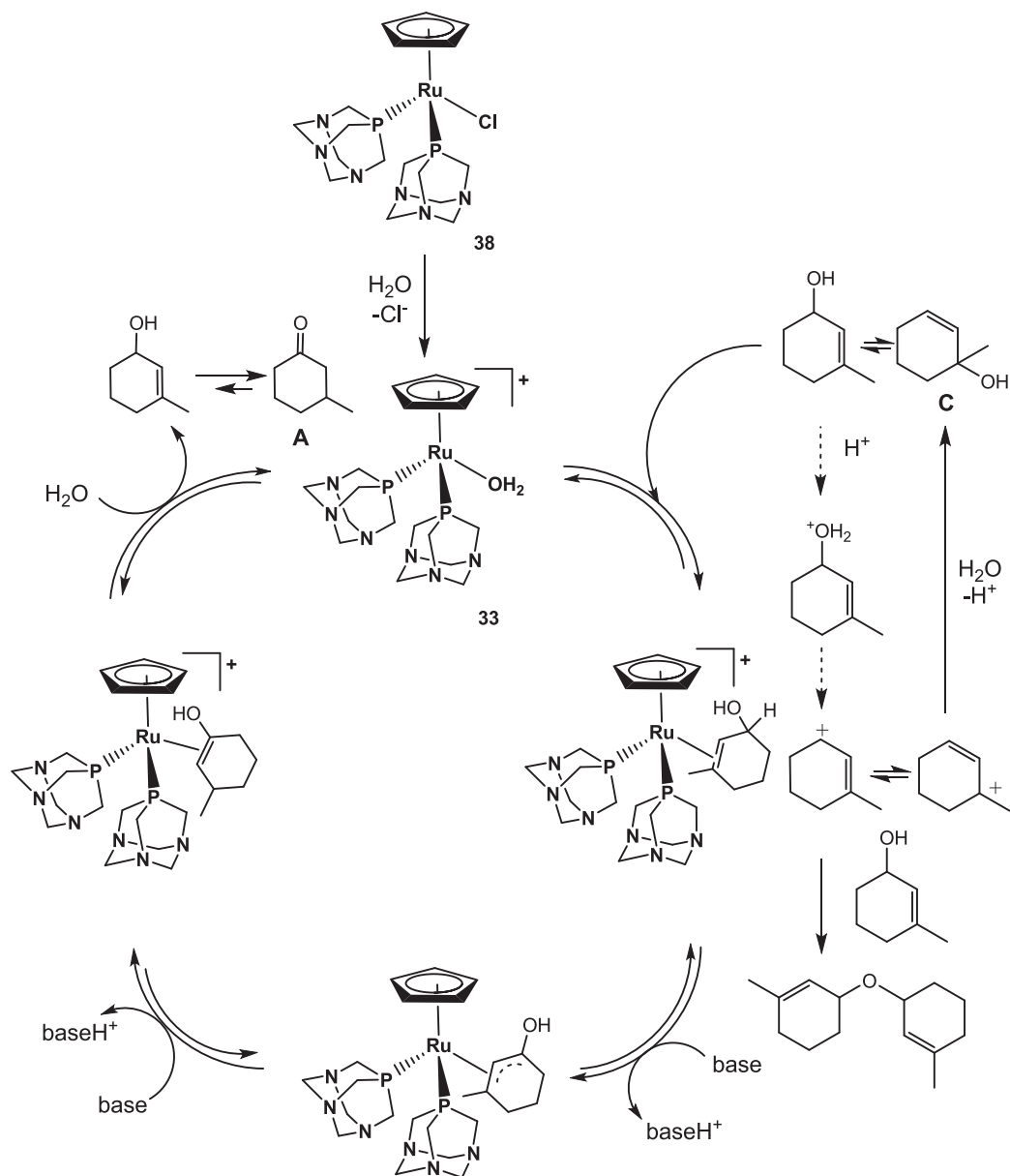


Fig. 11. Molecular drawings of complexes 36–38.



Scheme 18. Proposed catalytic mechanism for the isomerization and 1,3-transposition of 3-methyl-2-cyclohexen-1-ol in the presence of **33** [40].

was predominant (A:B=4:38). By replacing **38** with **33**, under the same reaction conditions **A** was largely the major product (70 %) under N₂. The effect was negligible under air, with similar results to those obtained with **38**. By carrying out a complete parameters screening, it was established that product distribution is mainly affected by the catalyst ratio, the solvent, and the atmosphere. In neat water, 10 mol% of catalyst give 3-methyl-2-cyclohexenone under aerobic conditions (TON=5.5), whereas at 1 mol%, 3-methylcyclohexanone is the preferred product under anaerobic conditions, with a better performance shown by precatalyst **33** (TON=70 vs. TON=36 with **38**). On the other hand, 1-methyl-2-cyclohexen-1-ol is the major product under aerobic conditions (44 %). For the isomerization process, catalyst **33** gave the best results, with the isomerization of 100 eq. of 3-methyl-2-cyclohexen-1-ol in biphasic cyclohexane/H₂O medium, with the possibility to recycle the catalyst confined in the water phase up to 5 times (overall TON=285). Also in this case, NMR studies with **33** revealed the formation of a reaction intermediate with η²-CH=CH coordination of the allylic alcohol to the metal. The proposed catalytic mechanism leading to **A** and **C** is shown in **Scheme 18**. Furthermore, the authors proposed that the

formation of oxidation product **B** may occur under air mediated by a Ru(III)-Ru(V) mechanism with the formation of an intermediate alkoxy-Ru species.

Among catalyzed reactions, the addition of water to unsaturated carbon-carbon or carbon-nitrogen triple bonds such as those present in alkynes and nitriles, is considered a useful and atom-efficient synthetic tool to produce ketones, aldehydes or amides, respectively.

In 2018, Caminade and coworkers described the application of dendrimer-supported RAPTA-type complexes for Ru-catalyzed phenylacetylene hydration to acetophenone (Markovnikov product) and 2-phenylacetaldehyde (*anti*-Markovnikov product) [41]. Dendrimers are hyperbranched macromolecules that can be obtained from a central core, using repetitive branching elements, starting from “Generation zero” (G₀) to the desired generation (G_n) upon consecutive branching steps. Using phosphorhydrazone as a core unit, dendrimers G₀-G₃ were obtained, terminating with a *N*-linked PTA unit, that was then used to coordinate [RuCl₂(p-cymene)] moieties. In this way, Ru-decorated catalytic materials could be obtained, with the number of Ru centers ranging from 6 to 48 (**Fig. 12**). The targets of the study were: i) to assess

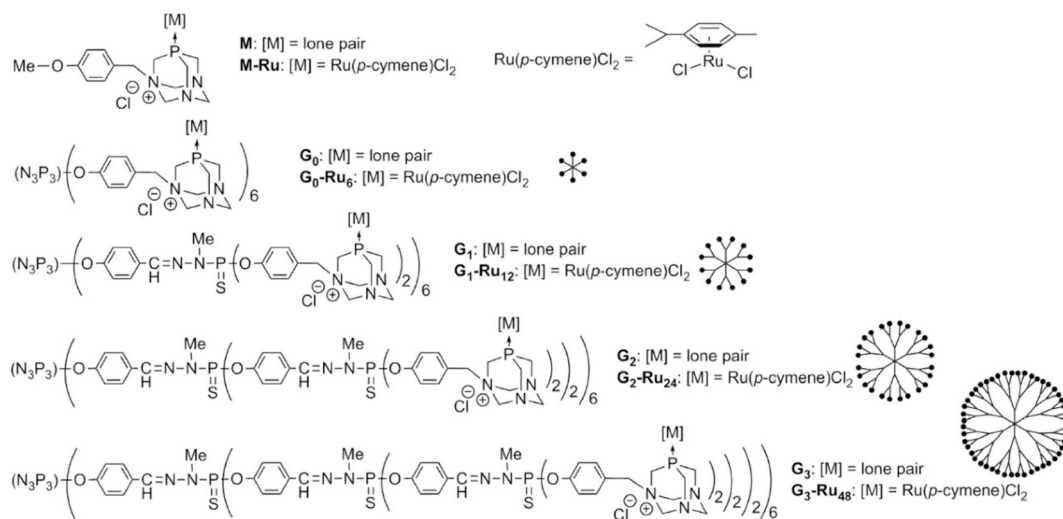
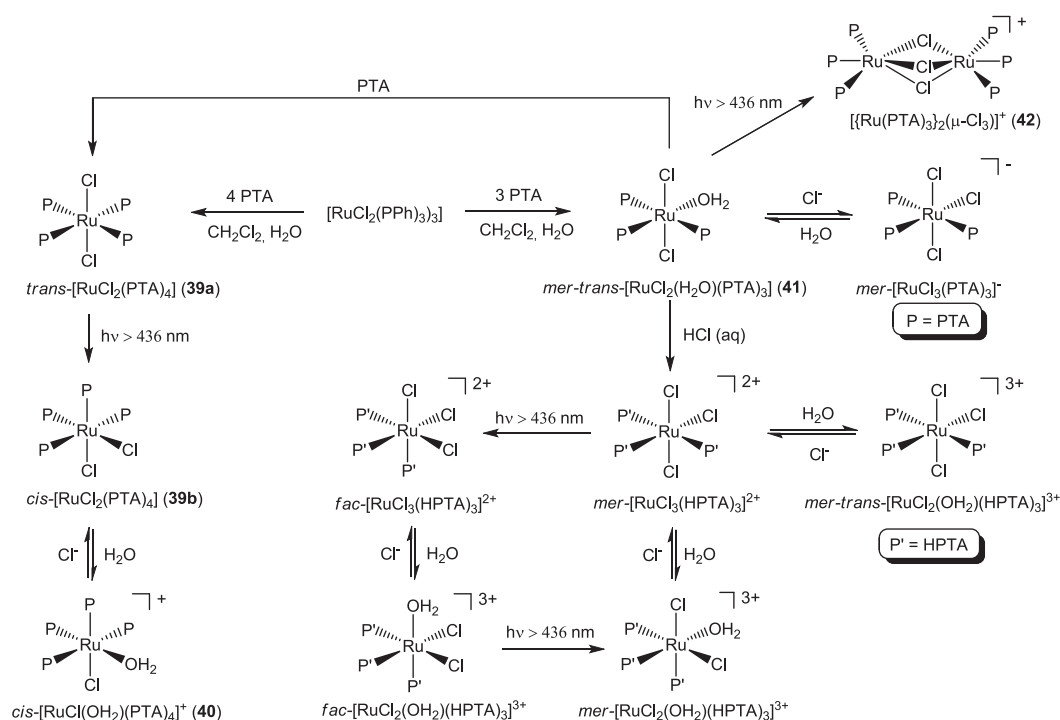


Fig. 12. Synthetic pathways for Ru-PTA decorated G₀-G₃ dendrimers. Reprinted from [41], with permission from Elsevier.



Scheme 19. Synthesis of complexes 39–42 and reactivity upon ligand exchange, protonation and light irradiation [42].

whether *in situ*-obtained catalysts could perform as the well-defined, synthesized dendrimer complexes, ii) the preference of Markovnikov vs. anti-Markovnikov addition, iii) catalyst recyclability. The catalytic tests started using the already synthesized complexes, in water/isopropanol (1:3), phenylacetylene:[Ru] = 100:5, 90 °C for 24–48 h. Under these conditions, very low conversions (14 %) were observed after 24 h, raising to 58 % after 48 h, with G₁-Ru₁₂. The system was improved by addition of an acid co-catalyst (H₂SO₄, 10 equiv.), and 26 % conversion was obtained with G₁-Ru₁₂ (1 mol% Ru) at 90 °C for 17 h. Next, *in situ* formed catalysts, formed by mixing G₁ with [RuCl₂(*p*-cymene)]₂ (1.1 equiv. Ru), were tested in the presence of H₂SO₄ (10 equiv.) at 90 °C for 17 h, surprisingly reaching a conversion of 68 %. Then, the effect of dendrimer generation was tested. Experiments were carried out with monomer M (+1 Ru) and dendrimer G₁ (+12 Ru). It was observed that with M, the main product of the catalysis was acetaldehyde (52 %

selectivity), whereas with G₁ the only product obtained was acetophenone (100 % selectivity). High conversions were observed at 90 °C, 17 h, with a better performance shown by the monomer (83 %) than the dendrimer (64 %). On the other hand, at 70 °C a slightly better performance was obtained with G₁. By comparison of M, G₁, and G₂ with Ru under these conditions, an almost linear increase of conversion with time (up to 109 h) was observed in all cases. The efficiency increased in the order G₂ < M < G₁, regardless of the duration of the experiment, and that was attributed to the so-called “dendritic effect”. Finally, catalyst recyclability (2 consecutive runs) was tested, comparing M and G₁ for 17 h at 90 °C, observing that the conversion slightly increased with M (from 83 to 87 %), and slightly decreased with G₁ (from 64 to 57 %).

The effect of visible light irradiation on the structural isomerization of some Ru-PTA complexes and its implications in catalytic reactions were studied by Kathó, Romerosa and coworkers in 2018 [42]. The

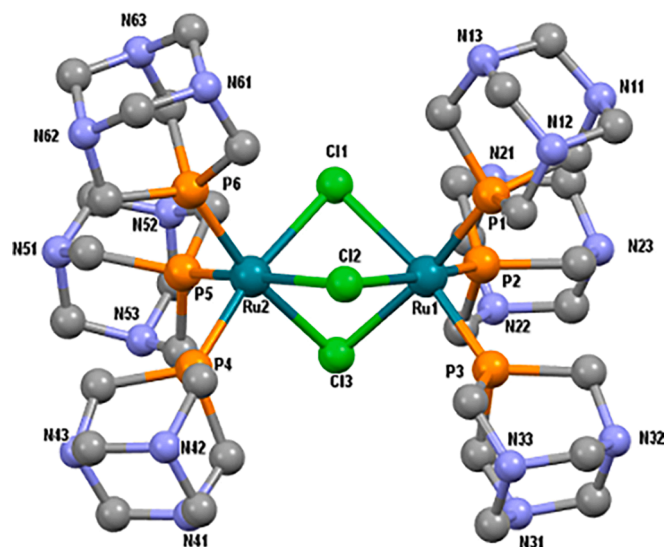


Fig. 13. X-ray crystal structure of complex $[\{\text{Ru}(\text{PTA})_3\}_2(\mu\text{-Cl}_3)]^+$ (42). Hydrogen atoms, solvent molecules and anions omitted for clarity. Drawings by CCDC Mercury® 3.9 [42].

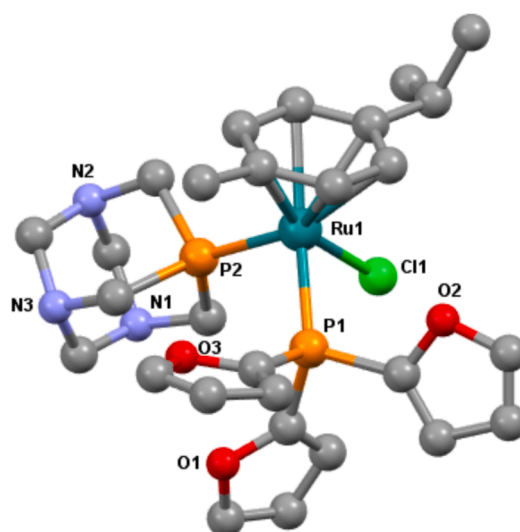


Fig. 14. X-ray crystal structures of complex $[\text{RuCl}(\eta^6\text{-cymene})(\text{PTA})(\text{PFu}_3)](\text{BF}_4)$ (43). Hydrogen atoms, solvent molecules and anions omitted for clarity. Drawings by CCDC Mercury® 3.9 [44].

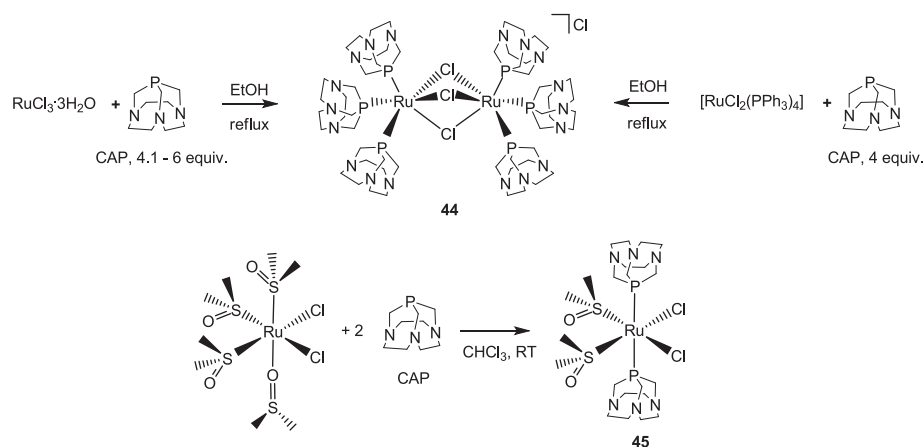
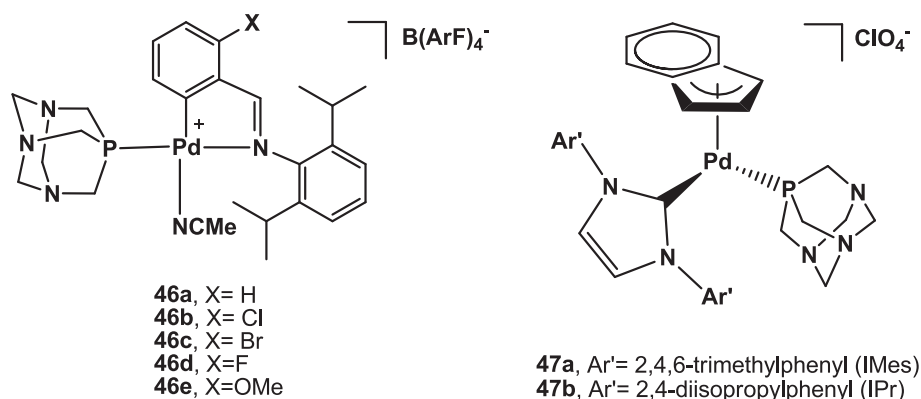
interest in this aspect stems from previous reports, highlighting that upon irradiation *trans*- $[\text{RuCl}_2(\text{PTA})_4]$ (39a) undergoes isomerization to *cis*- $[\text{RuCl}_2(\text{PTA})_4]$ (39b), to give then *cis*- $[\text{RuCl}(\text{OH}_2)(\text{PTA})_4]^+$ (40) upon $\text{H}_2\text{O}/\text{Cl}^-$ ligand exchange. Complex *mer-trans*- $[\text{RuCl}_2(\text{OH}_2)(\text{PTA})_3]$ (41) was obtained from the reaction of $[\text{RuCl}_2(\text{PPh}_3)_3]$ with PTA (3 equiv.) in a biphasic $\text{H}_2\text{O}/\text{CH}_2\text{Cl}_2$ mixture. As many reactions catalyzed by $[\text{RuCl}_2(\text{PTA})_4]$ have been carried out in the past without explicit exclusion of visible light (*i.e.* in the dark), the question arised on whether the light-triggered isomerization process might have an effect on catalytic results. The authors explored the reactivity pathways of 35–37 toward ligand substitution (aquation), protonation and visible light irradiation, obtaining various Ru-PTA and Ru-HPTA (HPTA=*N*-protonated PTA) products, as shown in Scheme 19. Furthermore, the use of $[\text{RuCl}_2(\text{dmsO})_4]$ (dmsO = dimethylsulfoxide) as synthetic precursor for Ru-PTA and Ru-(*N*-Bz-PTA) complexes was re-examined. Next, the effect of light on Ru-catalyzed cinnamaldehyde and benzaldehyde transfer hydrogenations was studied, typically by running the tests at 80 °C, 3 h, using HCO_2Na as the reducing agent. With 39a as catalyst, the results of the experiments performed in the dark were not different from those obtained under light, reaching high conversions and 100 % selectivity to cinnamol. In the case of benzaldehyde, complex 41 showed to be the most active catalyst (99 % conversion). The same complex also gave the best performance with cinnamaldehyde, with complete selectivity to cinnamol, albeit with lower conversion (55 %) than in the case of benzaldehyde. Lower conversions were obtained with complexes of the type $[\text{RuCl}_2(\text{dmsO})_2\text{L}_2]^{n+}$ (L=PTA, *n* = 0; *N*-Bz-PTA, *n* = 2). For this type of reaction, it was established that the effect of light on conversion and selectivity was negligible. Another example of catalytic application of this class of compounds was benzonitrile hydration to benzamide, for which previous studies showed good activity with catalysts formed *in situ* from 39b and PTA or (*N*-Bz-PTA). Interestingly, whereas *cis-cis-trans*- $[\text{RuCl}_2(\text{dmsO})_2(\text{PTA})_2]$ showed only modest catalytic activity after 3 h, even with the addition of 1 equiv. of free PTA, high conversion (99 %) was observed either with preformed or by *in situ* obtained *cis-cis-trans*- $[\text{RuCl}_2(\text{dmsO})_2(\text{N-Bz-PTA})_2]\text{Cl}_2$ (5 mol%, 100 °C, 1 h). Irradiation of 41 gave the bimetallic, chloride bridged complex $[\{\text{Ru}(\text{PTA})_3\}_2(\mu\text{-Cl}_3)]\text{Cl}$ (42). The solid state structure, obtained by single crystal X-ray diffraction analysis, is characterized by two octahedral Ru units, with three PTA ligands each and bridged by three chloride atoms (Fig. 13). When 42 was tested as catalyst for benzonitrile hydration, high conversions (81 %) were obtained after 1 h, that further increased in the

presence of added 2 equiv. of either PTA (96 % conversion) or *N*-Bz-PTA (99 %), respectively.

The use of 39a as catalyst for nitrile hydration reactions was further studied by Frost and coworkers in 2019, in detail by testing the possibility to obtain the catalytically active species *in situ*, by addition of PTA (1 to 15 equiv.) to $\text{RuCl}_3 \cdot 3\text{H}_2\text{O}$ (5 mol%), running the tests in neat water, 100 °C, in air, 7–24 h. [43] Results showed that using at least a Ru/PTA=1:6 ratio, comparable activities were observed between the pre-formed and the *in situ* obtained catalyst. Substrate scope screening showed that the catalyst is highly tolerant of different substituents on benzaldehyde, such as nitro, bromo, hydroxyl groups, it is also active for cyanopyridine and alkylnitriles, and that water phase at buffered pH=6.8 was ideal to achieve high conversions. Remarkable stability was shown by the *in situ* obtained system, as demonstrated by tests run for almost 100 days, using as low as 0.001 mol% of Ru (overall TON=22000, isolated yield of benzamide 22 %). Excellent catalyst recyclability (water phase) was also achieved, with up to 7 consecutive runs without significant activity decrease (GC conversions of ca. 99 %).

Vyas and coworkers compared the activity of three different Ru(*p*-cymene)-type complexes bearing tris(2-furyl)phosphine (PFu_3), namely $[\text{RuCl}_2(\eta^6\text{-cymene})(\text{PFu}_3)]$, $[\text{RuCl}(\eta^6\text{-cymene})(\text{PTA})(\text{PFu}_3)](\text{BF}_4)$ (43) and $[\text{RuCl}(\eta^6\text{-cymene})(\text{PFu}_3)_2](\text{BF}_4)$, for the hydration of different nitriles to amides in water under air, using 3 mol% of catalyst, 80 °C, 2–24 h [44]. Complex 43, obtained by PTA/chloride exchange reaction from $[\text{RuCl}_2(\eta^6\text{-cymene})(\text{PFu}_3)]$ in the presence of NaBF_4 , was also characterized in the solid state by single crystal X-ray diffraction methods, showing a piano-stool geometry with the *p*-cymene bound to Ru in a η^6 -fashion, one P-bound PTA ligand and one P-bound PFu_3 ligand (Fig. 14). The study showed that the bis(chloride)-Ru complex outperforms the two derivatives in terms of catalytic activity. A maximum yield of 70 % of benzamide was obtained after 12 h with 43 (5 mol%), whereas $[\text{RuCl}_2(\eta^6\text{-cymene})(\text{PFu}_3)]$ (3 mol%) achieved yields > 99 % after 4 h.

In our laboratories, the hydration of benzonitrile, 4-methylbenzonitrile and 2-pyridinecarbonitrile to the corresponding amides was tested in 2021 using catalytic systems obtained *in situ* from the novel complexes $[\{\text{Ru}(\text{CAP})_3\}_2(\mu\text{-Cl}_3)]\text{Cl}$ (44, CAP=1,4,7-triaza-9-phosphatricyclo[5.3.2.1]tridecane, Fig. 1) and *cis,cis,trans*- $[\text{RuCl}_2(\text{dmsO})_2(\text{CAP})_2]$ (45), shown in Scheme 20, with the addition of free CAP (2 equiv.) in neat water, 100 °C, 5–8 h, respectively [45]. Complex 44 could be obtained from the reaction of CAP with either $\text{RuCl}_3 \cdot 3\text{H}_2\text{O}$ (4.1 to 6 equiv. of CAP) or with $[\text{RuCl}_2(\text{PPh}_3)_4]$ (4 equiv. of

Scheme 20. Synthesis of Ru-CAP complexes **44** and **45** [45].Fig. 15. Molecular drawings of the novel palladacycle complexes **46** and the two [Pd(NHC)(PTA)(indenyl)]ClO₄ complexes **47**.

CAP) in CH₃CH₂OH under reflux conditions. Complex **45** was synthesized by addition of 2 equiv. of CAP to *cis*-[RuCl₂(dmsO)₄] in CHCl₃ at 25 °C. Initial catalytic tests of benzonitrile hydration to benzamide without the addition of the free ligand showed moderate conversions with **44** (35 %) and no conversion with **45**, whereas full conversion and selectivity were observed for both complexes in the presence of added CAP (0.02 mmol) after 5 h at 100 °C and a catalyst to substrate ratio 1:100. By decreasing the catalyst to substrate ratio to 1:250, after 8 h the system (**44** + 2 CAP) gave 89 % conversion (TON=222) and system (**45** + 2 CAP) reached 99 % conversion (TON=249). By further decrease of catalyst loading (1:500), system (**44** + 2 CAP) still showed some activity, with final conversion = 48 % after 24 h. In the case of 4-methylbenzonitrile, similar results to benzonitrile hydration were observed with 1 mol % of catalyst, and interestingly with a 1:250 catalyst:substrate ratio, system (**45** + 2 CAP) showed a better performance than system (**44** + 2 CAP) (56 % vs. 44 % conversion, 8 h). For 2-pyridinecarbonitrile, a particularly difficult substrate for catalytic hydration, system (**44** + 2 CAP) gave a maximum of 67 % conversion after 8 h at 100 °C with a substrate concentration of 0.07 M and up to 89 % with a substrate concentration of 0.20 M. Finally, catalyst recycling for system (**44** + 2 CAP, 1 mol%, 6 h for each run) was demonstrated for benzonitrile hydration, showing at least five consecutive runs without apparent loss of activity.

3.3. Palladium

The five cationic palladium(II) complexes **46a-e** depicted in Fig. 15, bearing PTA, MeCN and several substituted benzylidene-2,6-diisopropylphenylamines ((R-C₆H₃)CH=N{2,6-ⁱPr₂-C₆H₃}) as

Table 4
Phenylacetylene polymerization catalyzed by palladacycle complexes

Catalyst	Solvent	T (°C)	TON ^b	Productivity ^c	M _w ^d
46a	THF	60	4400	41.3	2440
46b	THF	60	4533	42.6	2515
46c	THF	60	2853	26.8	2362
46d	THF	60	4850	45.6	2656
46e	THF	60	4203	39.5	2557
46d	THF	25	3016	28.3	4175
46d	DCM	60	3180	29.9	1133
46d	Toluene	60	2480	23.3	1046
42d	MeCN	60	2050	19.3	1249
42d	DCM/MeCN (9:1)	60	3883	36.5	4190
46d	DCM/MeCN (7:1)	60	3550	33.4	4429

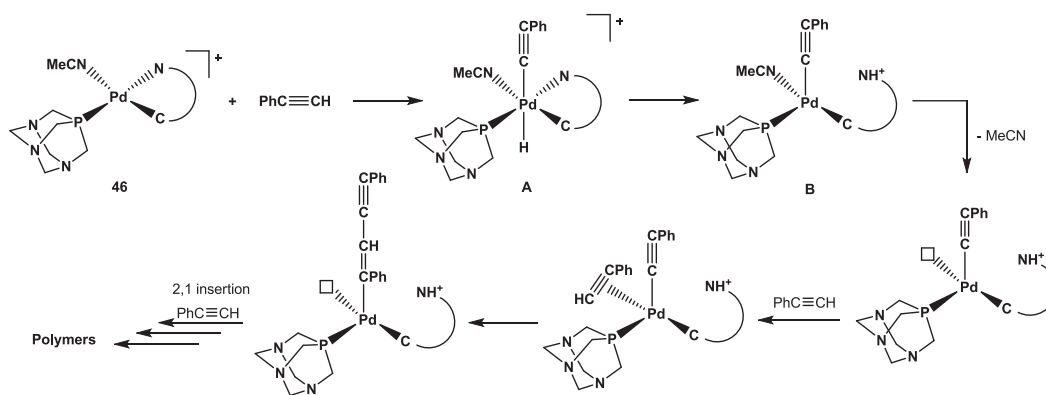
^a Reaction conditions: substrate: Pd = 50:1, [Pd] = 3 mM, 48 h, solvent 10 mL.

^b g of product per mol of Pd.

^c g of product per g of Pd.

^d Weight average molecular weight of methanol insoluble product.

coordinating ligands, were prepared by treatment of the corresponding neutral palladacycles of formula [PdCl(PTA)(R-C₆H₃)CH=N{2,6-ⁱPr₂-C₆H₃}] with NaB(ArF)₄ (sodium *tetrakis*[3,5-bis(trifluoromethyl)-phenyl] borate) in acetonitrile [46]. All these compounds differ from each other depending on the nature of the *meta*-substituents on the cyclometalated



Scheme 21. Proposed mechanism for phenylacetylene polymerization catalyzed by cationic palladacycle complexes **46**.

ring, but the presence of only one singlet in the $^{31}\text{P}\{^1\text{H}\}$ NMR spectra of compounds in deuterated solutions was indicative of the formation of only one isomer in all cases. This was also confirmed by the X-ray diffraction analysis of single crystals obtained for complex **46e** revealing a slightly distorted square-planar geometry around the metal with the phosphine in *trans* position to the imine nitrogen atom.

Complexes **46** were tested as catalyst precursors in the polymerization of phenylacetylene under the optimized reaction conditions reported in Table 4. With the exception of complex **46c**, all compounds showed high conversions by running the reactions in THF at 60 °C, with TONs > 4200 and productivity values > 40. The presence of a more electron-withdrawing substituent in the complex increased the catalyst activity, although **46b** and **46c**, containing chloro or bromo substituents, respectively, showed different results. Indeed, the productivity of **46b** resulted of 42.6 while that of **46c** was only of 26.8 under the same reaction conditions. The lower activity of **46c** was attributed by the authors to its low stability in solution likely due to the steric hindrance of the bromo substituent which may hinder the coordination of the *ortho*-imine group to the metal center, thus resulting in a weaker Pd-N bond. Being the PTA-based fluoro complex **46d** the most active catalyst, the polymerization of phenylacetylene was further tested with this compound in THF at room temperature, resulting in lower values of TON (3016 at 25 °C vs 4850 at 60 °C) and productivity (28.3 at 25 °C vs 45.6 at 60 °C), but producing polymers with higher molecular weights (4175 at 25 °C vs 2656 at 60 °C). Furthermore, the effect of solvent was also investigated with **46d** by performing the reaction at 60 °C in toluene, MeCN, CH_2Cl_2 , or mixtures of these latter. In all test, the conversions were lower than those observed in THF under the same conditions, indicating that a coordinating solvent such as THF has a role in the

reaction mechanism stabilizing the coordinatively unsaturated metal complex.

Based on results of studies on phenylacetylene polymerization previously reported in the literature and by performing NMR experiments with complex **46d** in THF- d_6 under pseudo catalytic reaction conditions, a mechanism of the catalytic cycle has been proposed by the authors (Scheme 21) [46]. This consists of an initial oxidative addition of the substrate to the cationic palladium(II) precursor producing a σ -alkynyl-Pd-hydride species A, which then undergoes reductive elimination, with the imine moiety and the hydride combining to give species B. The following dissociation of MeCN allows the phenylacetylene coordination to Pd in η^2 -fashion followed by the insertion of the alkyne into the Pd-alkynyl σ -bond. Further alkyne coordination and insertion steps produce the chain propagation.

Very recently, two new cationic palladium(II) indenyl complexes **47a** and **47b** bearing one PTA and one NHC ligand (where NHC=N-heterocyclic carbene), have been reported by Scattolin, Visentin and coworkers (Fig. 15) [47]. These compounds were synthesized in high yields starting from the neutral precursors $[\text{PdCl}(\text{NHC})(\text{indenyl})]$ (where NHC is IMes for **47a** and IPr for **47b**), and characterized in solution by NMR spectroscopy and in the solid state by single crystal X-ray diffraction (Fig. 16). In both cases, the structures feature a pseudo-piano stool geometry, occupied by the indenyl ligand (stool), one PTA and one NHC ligand (two legs). As for other palladium-NHC complexes, **47a** and **47b** were tested as precatalysts for the Suzuki-Miyaura coupling of 4-bromo and 4-chloroacetophenones with phenylboronic acid in aqueous media at 80 °C. The first catalytic reactions were carried out with 4-bromoacetophenone as the model substrate in the presence of tetrabutylammonium bromide (TBAB, 1.5 eq.) and K_2CO_3 (1.5 eq.) as

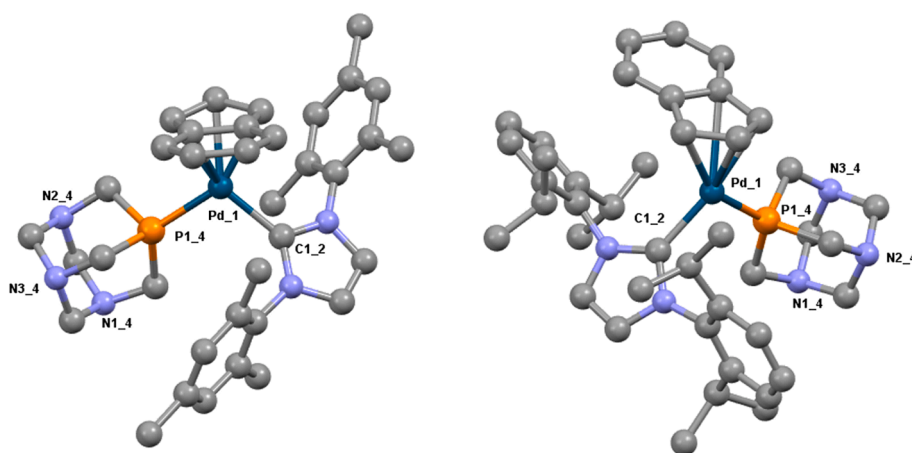
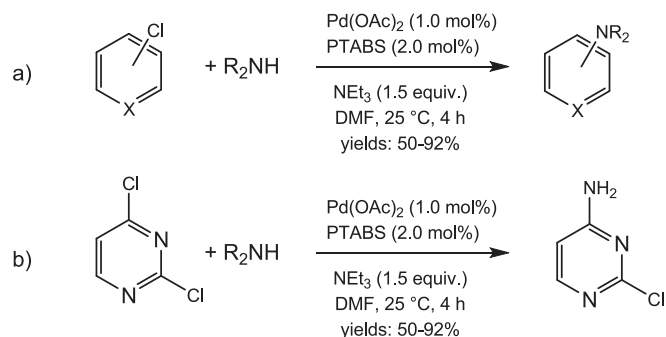
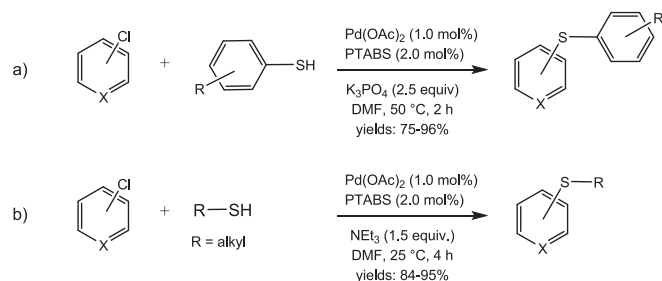


Fig. 16. X-ray crystal structures of $[\text{Pd}(\text{PTA})(\text{NHC})(\text{indenyl})]$ complexes **47a** (left) and **47b** (right). Hydrogen atoms, solvent molecules and anions omitted for clarity. Drawings by CCDC Mercury® 3.9 [47].

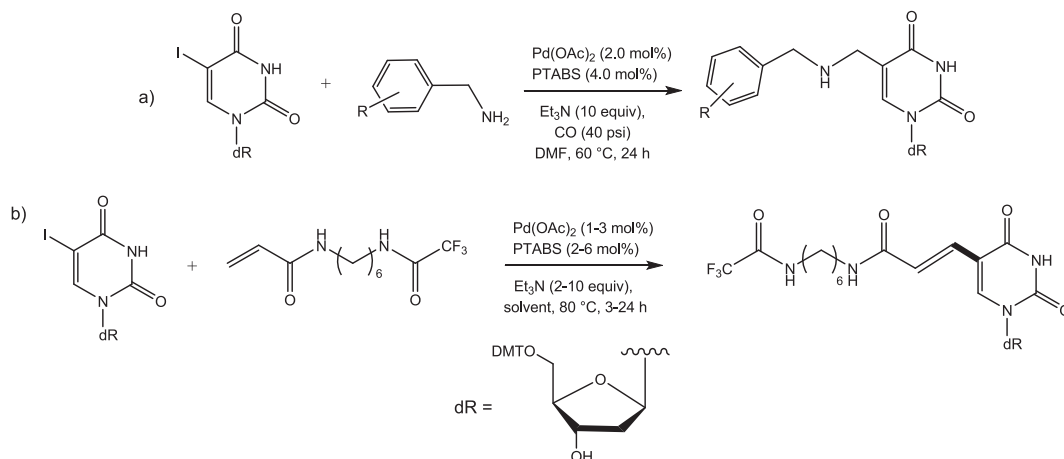


Scheme 22. Chloroheteroarenes amination /monoamination catalyzed by Pd/PTABS [49].



Scheme 23. Thioetherification of chloroheteroarenes catalyzed by Pd/PTABS [50].

the base. With a 1 mol% catalyst loading, the best performance was observed with complex **47a** producing [1,1'-biphenyl]-4-yl acetate in 94 % yield after 21 h. A yield of 87 % was obtained with **47b** under the same conditions. By reducing the catalyst loading to 0.1 mol%, a conversion of 88 % was observed with **47a** after only 2 h. Furthermore, yields > 80 % were reached under the same reaction conditions with catalyst **47a** in three recycle experiments performed by extracting the products in ethyl acetate and adding fresh substrates and TBAB to the aqueous solution from the previous cycle containing the catalyst. Very good catalytic performances ranging from 41 to 98 % were observed again with **47a** in the reaction of different aryl bromides and arylboronic acids and the same catalyst resulted active also with the more challenging 4-chloroacetophenone as substrate. In detail, by reacting 4-chloroacetophenone with phenylboronic acid in water at 80 °C for 24 h, conversions of 34 % and 77 % were obtained with 0.1 and 1 mol% catalyst loading, respectively [47].



Scheme 24. Aminocarbonylation and Heck-type reactions catalyzed by Pd/PTABS [51,52].

In addition to well-defined Pd complexes bearing PTA and derivatives, efficient catalysts were obtained *in situ* by combination of Pd (II) precursors with PTABS (KapdiPhos, Fig. 1). These catalytic systems were applied by Kapdi and coworkers for C-element coupling reactions such as Buchwald-Hartwig and Heck-type reactions, and the results have been summarized in excellent review articles [48]. In 2018, the system based on Pd(OAc)₂ (1 mol%), PTABS (2 mol%), NEt₃ (1.5 equiv.), DMF, 25 °C, 4 h, was applied for the selective, room temperature amination of chloroheteroarenes using secondary amines such as piperidine, pyrrolidine, and several others (Scheme 22a, >35 examples overall reported) with yields up to 93 % [49]. Monoamination of 2,4-dichloropyrimidine with four different secondary amines, namely, pyrrolidine, piperidine, morpholine, and piperazine derivatives was also demonstrated to occur selectively at the 4-position, with the advantage of leaving the 2-chloro position available for further synthetic modifications (Scheme 22b).

A year later, C–S bond-making reactions of aryl- and heteroaryl chlorides with arylthiols and alkylthiols in the presence of Pd/PTABS was demonstrated by Kapdi, Schutzke and coworkers [50]. Under optimized conditions (1.0 mmol of chloroheteroarene, 1.5 mmol of thiol, 1.0 mol % Pd(OAc)₂, 2.0 mol % PTABS ligand, 3.0 mL DMF, 50 °C, 2 h), numerous examples of successful C–S couplings were reported, with isolated yields in the range 75–96 % for thiophenols (Scheme 23a) and 84–95 % for alkanethiols (Scheme 23b). Thioetherification of synthons of pharmaceutical interest such as chloropyrimidines, purines and ribonucleosides was also demonstrated.

Next, the versatility of the Pd/PTABS system in organic synthesis was extended by the same authors to aminocarbonylation reactions, in detail using a idonucleoside as substrate, a (substituted) primary benzylamine and CO gas at 60 °C. It was shown that the protocol is suitable for a wide range of amines, including (heteroaryl)benzylic, aliphatic acyclic, alicyclic and secondary amines [51], shown in Scheme 24a. More recently, the same authors applied this protocol to a Heck-type alkenylation reaction for the multi-gram scale (>100 g) synthesis of the amino-modifier nucleoside 'Ruth Linker' [52], see Scheme 24b. This is a C5 pyrimidine modified nucleoside analogue that finds use in pharmaceutical industry for the incorporation of a primary amine in a synthetic oligonucleotide, that can be useful for non-radioactive labeling, detection of biomolecules, and assembly of COVID-19 test kits. The Pd/PTABS protocol was shown to bring about the synthesis of the desired product at low catalyst concentration, with column-free isolation, high product purity, reproducibility, and shorter reaction time.

4. Conclusions and outlook

In conclusion, the present literature summary shows that the design and synthesis of water-soluble ligands and related coordination

compounds for use in homogeneous and heterogeneous catalysis is still a field of interest for the chemistry community, with numerous contributions published in the period 2018–2024 so far. Remarkable catalytic activities were obtained, and in some cases important aspects such as efficient catalyst recyclability and the use of either neat water or biphasic water/organic solvent media were demonstrated, representing the strongest features in favor of this approach to catalysis. Next, recent reports highlighted the use of PTA-type aminophosphines not only as stabilizing ligands for well-defined metal complexes, but also as scaffolds for 1D-3D networks and Metal Organic Frameworks (MOF), that were as well applied in catalytic applications. In perspective, in our opinion this field of research may still contribute interesting results, in particular in the growing area of novel earth-abundant metal molecular complexes and materials, to increase the number of applications and process sustainability, by replacement of costly precious metals where possible.

CRedit authorship contribution statement

Antonella Guerriero: Conceptualization, Data curation, Writing – original draft, Writing – review & editing. **Luca Gonsalvi:** Conceptualization, Data curation, Writing – original draft, Writing – review & editing.

Declaration of competing interest

The authors declare that they have no known competing financial interests or personal relationships that could have appeared to influence the work reported in this paper.

Data availability

No data was used for the research described in the article.

References

- [1] P. T. Anastas, W. Leitner, P. G. Jessop, J.-C. Li, P. Wasserscheid, A. Stark, Handbook of green chemistry: green solvents, Eds Wiley-VCH: Weinheim, Germany, 2010.
- [2] F. Kerton, R. Marriott, Alternative solvents for green chemistry, 2nd Edition RSC Green Chemistry Series 20 (2013) 1–350, <https://doi.org/10.1039/9781849736824>.
- [3] K.H. Shaughnessy, Hydrophilic Ligands and Their Application in Aqueous-Phase Metal-Catalyzed Reactions, *Chem. Rev.* 109 (2009) 643–710, <https://doi.org/10.1021/cr800403r>.
- [4] a) A.D. Phillips, L. Gonsalvi, A. Romerosa, F. Vizza, M. Peruzzini, Coordination Chemistry of 1,3,5-triaza-7-phosphatricyclo[3.3.1.1]decane (PTA) Transition metal complexes and related catalytic, medicinal and photoluminescent applications, *Coord. Chem. Rev.* 248 (2004) 955–993, <https://doi.org/10.1016/j.ccr.2004.03.010>;
b) J. Bravo, S. Bolano, L. Gonsalvi, M. Peruzzini, Coordination chemistry of 1,3,5-triaza-7-phosphaadamantane (PTA) and derivatives. Part II. The quest for tailored ligands, complexes and related applications, *Coord. Chem. Rev.* 254 (2010) 555–607, <https://doi.org/10.1016/j.ccr.2009.08.006>;
c) A. Guerriero, M. Peruzzini, L. Gonsalvi, Coordination Chemistry of 1,3,5-triaza-7-phosphatricyclo[3.3.1.1]decane (PTA) and derivatives. Part III. Variations on a theme: Novel architectures, materials and applications, *Coord. Chem. Rev.* 355 (2018) 328–361, <https://doi.org/10.1016/j.ccr.2017.09.024>.
- [5] L. Gonsalvi, A. Guerriero, F. Hapiot, D.A. Krogstad, E. Monflier, G. Reginato, M. Peruzzini, Lower- and upper-rim-modified derivatives of 1,3,5-triaza-7-phosphaadamantane: Coordination chemistry and applications in catalytic reactions in water, *Pure Appl. Chem* 85 (2013) 385–396, <https://doi.org/10.1351/PAC-CON-12-07-10>.
- [6] S.N. Britvin, A. Lotnyk, Water-soluble phosphine capable of dissolving elemental gold: the missed link between 1,3,5-triaza-7-phosphaadamantane (PTA) and Verkade's ephemeral Ligand, *J. Am. Chem. Soc.* 137 (2015) 5526–5535, <https://doi.org/10.1021/jacs.5b01851>.
- [7] a) S. Swaminathan, R. Karvembu, Dichloro Ru(II)-p-cymene-1,3,5-triaza-7-phosphaadamantane (RAPTA-C): A Case Study, *ACS Pharmacol. Transl. Sci.* 6 (2023) 982–996, <https://doi.org/10.1021/acspctsci.3c00085>;
b) F. Scalambra, P. Lorenzo-Luis, I. de los Ríos, A. Romerosa, New Findings in Metal Complexes with Antiproliferative Activity Containing 1,3,5-Triaza-7-phosphaadamantane (PTA) and Derivative Ligands, *Eur. J. Inorg. Chem.* (2019) 1529–1538, <https://doi.org/10.1002/ejic.201801426>;
c) M. Rausch, P.J. Dyson, P. Nowak-Sliwinska, Recent Considerations in the Application of RAPTA-C for Cancer Treatment and Perspectives for Its Combination with Immunotherapies, *Adv. Therap.* 2 (2019) 1900042, <https://doi.org/10.1002/adtp.201900042>.
- [8] a) S.W. Jaros, M. Florek, B. Bażanów, J. Panek, A. Krogul-Sobczak, M.C. Oliveira, J. Król, U. Śliwińska-Hill, D.S. Nesterov, A.M. Kirillov, P. Smoleński, Silver Coordination Polymers Driven by Adamantoid Blocks for Advanced Antiviral and Antibacterial Biomaterials, *ACS Appl. Mater. Interfaces* 16 (2024) 13411–13421, <https://doi.org/10.1021/acsmi.3c15606>;
b) P. Smoleński, Coordination Engineering with 1,3,5-Triaza-7-Phosphaadamantane (PTA) towards Biologically Active Silver-Organic Frameworks, Chapter 5 in *Ligands: Synthesis, Characterization and Role in Biotechnology* ISBN (2014), 978-1-63117-143-7;
c) A.M. Kirillov, S.W. Wiecezorek, M.F.C. Guedes da Silva, J. Sokolnicki, P. Smoleński, A.J.L. Pombeiro, Crystall engineering with 1,3,5-triaza-7-phosphaadamantane (PTA): first PTA-driven 3D metal-organic frameworks, *CrystEngComm* 13 (2013) 6329–6333, <https://doi.org/10.1039/C3CE05612C>.
- [9] A. Udvardy, F. Joó, A. Kathó, Synthesis and catalytic applications of Ru(II)-phosphatropine complexes with the use of simple water-soluble Ru(II)-precursors, *Coord. Chem. Rev.* 438 (2021) 213871, <https://doi.org/10.1016/j.ccr.2021.213871>.
- [10] A. Guerriero, L. Gonsalvi, From traditional PTA to novel CAP: A comparison between two adamantane cage-type aminophosphines, *Inorg. Chim. Acta* 518 (2021) 120251, <https://doi.org/10.1016/j.ica.2021.120251>.
- [11] T. Agarwal, S. Kaur-Ghumaan, Mono- and dinuclear mimics of the [FeFe] hydrogenase enzyme featuring bis(monothiolato) and 1,3,5-triaza-7-phosphaadamantane ligands, *Inorg. Chim. Acta* 504 (2020) 119442, <https://doi.org/10.1016/j.ica.2020.119442>.
- [12] a) B.J. Frost, C.M. Bautista, R. Huang, J. Shearer, Manganese complexes of 1,3,5-Triaza-7-phosphaadamantane (PTA): the first nitrogen-bound transition-metal complex of PTA, *Inorg. Chem.* 45 (2006) 3481–3483, <https://doi.org/10.1021/ic060322p>;
b) F. Mohr, J. Nielsen, U. Schatzschneider, C.W. Lehmann, Synthesis, Structures, and CO Releasing Properties of two Tricarbonyl Manganese(I) Complexes, *Z. Anorg. Allg. Chem.* 638 (2012) 543–546, <https://doi.org/10.1002/zaac.201100422>.
- [13] V. Kaim, S. Kaur-Ghumaan, Mononuclear Mn complexes featuring N, S-/N, N-donor and 1,3,5-triaza-7-phosphaadamantane ligands: synthesis and electrocatalytic properties, *New. J. Chem.* 45 (2021) 20272–20279, <https://doi.org/10.1039/d1nj02104d>.
- [14] E.I. Śliwa, D.S. Nesterov, J. Klak, P. Jakimowicz, A.M. Kirillov, P. Smoleński, Unique copper-organic networks self-assembled from 1,3,5-triaza-7-phosphaadamantane and its oxide: synthesis, structural features, and magnetic and catalytic properties, *Cryst. Growth Des.* 18 (2018) 281–2823, <https://doi.org/10.1021/acs.cgd.7b01581>.
- [15] E.I. Śliwa, D.S. Nesterov, M. Kirillova, J. Klak, A.M. Kirillov, P. Smoleński, A 3D MOF based on adamantoid tetracopper(II) and aminophosphine oxide cages: structural features and magnetic and catalytic properties, *Inorg. Chem.* 60 (2021) 9631–9644, <https://doi.org/10.1021/acs.inorgchem.1c00868>.
- [16] A.G. Mahmoud, M.F.C. Guedes da Silva, J. Sokolnicki, P. Smoleński, A.J. L. Pombeiro, Hydrosoluble Cu(I)-DAPTA complexes: synthesis, characterization, luminescence thermochromism and catalytic activity for microwave-assisted three-component azide-alkyne cycloaddition click reaction, *Dalton Trans.* 47 (2018) 7290–7299, <https://doi.org/10.1039/c8dt01232f>.
- [17] A.G. Mahmoud, M.F.C. Guedes da Silva, E.I. Śliwa, P. Smoleński, M.L. Kuznetsov, A.J.L. Pombeiro, Copper(II) and sodium(I) complexes based on 3,7-diacetyl-1,3,7-triaza-5-phosphabicyclo[3.3.1]nonane-5-oxide: synthesis, characterization, and catalytic activity, *Chem. Asian. J.* 13 (2018) 2868–2880, <https://doi.org/10.1002/asia.201800799>.
- [18] V.I. Siele, Some reactions of 1,3,5-triaza-7-phosphaadamantane and its 7-oxide, *J. Heterocycl. Chem.* 14 (1977) 337–339, <https://doi.org/10.1002/jhet.5570140238>.
- [19] A.G. Mahmoud, P. Smoleński, M.F.C. Guedes da Silva, A.J.L. Pombeiro, Water-soluble O-, S- and Se-functionalized cyclic acetyl-triaza-phosphines. Synthesis, characterization and application in catalytic azide-alkyne cycloaddition, *Molecules* 25 (2020) 5479, <https://doi.org/10.3390/molecules25225479>.
- [20] I.L. Librando, A.G. Mahmoud, S.A.C. Carabineiro, M.F.C. Guedes da Silva, C.F.G. C. Geraldes, A.J.L. Pombeiro, Synthesis of a novel series of Cu(I) complexes bearing alkylated 1,3,5-triaza-7-phosphaadamantane as homogeneous and carbon-supported catalysts for the synthesis of 1- and 2-substituted-1,2,3-triazoles, *Nanomaterials* 11 (2021) 2702, <https://doi.org/10.3390/nano11102702>.
- [21] A.M. Kirillov, P. Smoleński, M. Haukka, M.F.C. Guedes da Silva, A.J.L. Pombeiro, Unprecedented metal-free C(sp³)-C(sp³) bond cleavage: switching from N-Alkyl- to N-Methyl-1,3,5-triaza-7-phosphaadamantane, *Organometallics* 28 (2009) 1683–1687, <https://doi.org/10.1021/om801026a>.
- [22] U. Parmar, D. Somvanshi, S. Kori, A.A. Desai, R. Dandela, D.K. Maity, A.R. Kapdi, Room-temperature amination of chloroheteroarenes in water by a recyclable copper(II)-phosphaadamantane sulfonate system, *J. Org. Chem.* 86 (2021) 8900–8925, <https://doi.org/10.1021/acs.joc.2020.1c00845>.
- [23] H. Shet, M. Patel, J.M. Waikar, P.M. More, Y.S. Sanghvi, A.R. Kapdi, *Chem. Asian. J.* 18 (2023) e202201006, <https://doi.org/10.1002/asia.202201006>.
- [24] A.G. Mahmoud, I.L. Librando, A. Paul, S.A.C. Carabineiro, A.M. Ferrara, A. M. Botelho do Rego, M.F.C. Guedes da Silva, C.F.G.C. Geraldes, A.J.L. Pombeiro, Novel organotin-PTA complexes supported on mesoporous carbon materials as recyclable catalysts for solvent-free cyanosilylation of aldehydes, *Catalysis Today* 423 (2023) 114270, <https://doi.org/10.1016/j.cattod.2023.114270>.
- [25] a) D.S. Ramarou, B.C.E. Makhubela, G.S. Smith, Synthesis of Rh(I) alkylated-PTA complexes as catalyst precursors in the aqueous-biphasic hydroformylation of 1-

- octene, *J. Organomet. Chem.* 870 (2018) 23–31, <https://doi.org/10.1016/j.jorganchem.2018.05.019>;
- b) A. Udvardy, A.C. Bényei, P. Juhász, F. Joó, Á. Kathó, Two in one: Charged tertiary phosphines held together by ionic or covalent interactions as bidentate phosphorus ligands for synthesis of half-sandwich Ru(II)-complexes, *Polyhedron* 60 (2013) 1–9, <https://doi.org/10.1016/j.poly.2013.05.008>.
- [26] R.S. Prajapati, A.R. Kapdi, R. Sahu, B.M. Bhanage, Selectivity tuning using Rh/PTABS catalytic system for the hydroformylation of eugenol, *Catal. Today* 438 (2024) 114804, <https://doi.org/10.1016/j.cattod.2024.114804>.
- [27] K. Hua, X. Liu, B. Wei, Z. Shao, Y. Deng, L. Zhong, H. Wang, Y. Sun, Chemo- and regioselective hydroformylation of alkenes with CO₂/H₂ over a bifunctional catalyst, *Green Chem.* 23 (2021) 8040–8046, <https://doi.org/10.1039/d0gc03913f>.
- [28] K. Hua, X. Liu, J. Chen, B. Wei, H. Wang, Y. Sun, Regioselective hydroxymethylation of alkenes to linear alcohols with CO₂/H₂ using a Rh/Ru dual catalyst, *ACS Sustainable Chem. Eng.* 9 (2021) 16741–16748, <https://doi.org/10.1021/acssuschemeng.1c06057>.
- [29] a) M. Trivedi, P. Sharma, I.K. Pandey, A. Kumar, S. Kumar, N.P. Rath, Acid-assisted hydrogenation of CO₂ to methanol using Ru(II) and Rh(III) RAPTA-type catalysts under mild conditions, *Chem. Commun.* 57 (2021) 8941–8944, <https://doi.org/10.1039/d1cc03049c>;
- b) A. Dorcier, W.H. Ang, S. Bolaño, L. Gonsalvi, L. Juillerat-Jeannerat, G. Laurency, M. Peruzzini, A.D. Phillips, F. Zanobini, P.J. Dyson, In vitro evaluation of rhodium and osmium rapta analogues: the case for organometallic anticancer drugs not based on ruthenium, *Organometallics* 25 (2006) 4090–4096, <https://doi.org/10.1021/om060394e>;
- c) S. Bolaño, A. Albinati, J. Bravo, M. Caporali, L. Gonsalvi, L. Male, M. M. Rodríguez-Rocha, A. Rossin, M. Peruzzini, Synthesis and reactivity of rhodium (III) pentamethylcyclopentadienyl complexes of N-B-PTA(BH₃): X-ray crystal structures of [Cp**Rh*Cl₂{N-B-PTA(BH₃)}] and [Cp**Rh*{N-B-PTA(BH₃)}(η²-CH₂=CHPh)], *J. Organomet. Chem.* 693 (2008) 2397–2406, <https://doi.org/10.1016/j.jorganchem.2008.04.006>;
- d) C.S. Allardyce, P.J. Dyson, D.J. Ellis, S.L. Heath, Ru(η⁶-p-cymene)Cl₂(pta) [pta = 1,3,5-triaza-7-phosphatricyclo-[3.3.1.1]decane]: a water soluble compound that exhibits pH dependent DNA binding providing selectivity for diseased cells, *Chem. Commun.* (2001) 1396–1397, <https://doi.org/10.1039/B104021A>.
- [30] C.E. Czégényi, M. Fekete, E. Tóbiás, A. Udvardy, H. Horváth, G. Papp, F. Joó, Redox isomerization of allylic alcohols catalyzed by new water-soluble Rh(I)-N-heterocyclic carbene complexes, *Catalysts* 10 (2020) 1361, <https://doi.org/10.3390/catal10111361>.
- [31] C. Fink, L. Chen, G. Laurency, Homogeneous catalytic formic acid dehydrogenation in aqueous solution using ruthenium arene phosphine catalysts, *Z. Anorg. Allg. Chem.* 644 (2018) 740–744, <https://doi.org/10.1002/zaac.201800107>.
- [32] A. Bhatia, S. Muthaiah, Well-defined ruthenium complex for acceptorless alcohol dehydrogenation in aqueous medium, *ChemistrySelect* 3 (2018) 3737–3741, <https://doi.org/10.1002/slct.201702981>.
- [33] A. Bhatia, S. Muthaiah, Synthesis of a water-soluble ruthenium complex and its catalytic activity for acceptorless alcohol dehydrogenation in aqueous medium, *Synlett* 29 (2018) 1644–1648, <https://doi.org/10.1055/s-0037-1610177>.
- [34] A. Bhatia, M. Kannan, S. Muthaiah, Ruthenium-Promoted Acceptorless and Oxidant-Free Lactone Synthesis in Aqueous Medium, *Synlett* 30 (2019) 721–725, <https://doi.org/10.1055/s-0037-1612247>.
- [35] N. Marozsán, H. Horváth, É. Kovács, A. Udvardy, A. Erdei, M. Purgel, F. Joó, Catalytic racemization of secondary alcohols with new (arene)Ru(II)-NHC and (arene)Ru(II)-NHC-tertiary phosphine complexes, *Mol. Catal.* 445 (2018) 248–256, <https://doi.org/10.1016/j.mcat.2017.11.040>.
- [36] F. Scalambra, P. Lorenzo-Luis, I. de los Ríos, A. Romerosa, Isomerization of allylic alcohols in water catalyzed by transition metal complexes, *Coord. Chem. Rev.* 393 (2019) 118–148, <https://doi.org/10.1016/j.ccr.2019.04.012>.
- [37] F. Scalambra, N. Holzmann, L. Bernasconi, S. Imberti, A. Romerosa, Water participation in catalysis: an atomistic approach to solvent effects in the catalytic isomerization of allylic alcohols, *ACS Catal.* 8 (2018) 3812–3819, <https://doi.org/10.1021/acscatal.8b00199>.
- [38] F. Scalambra, B. Lopez-Sanchez, L. Ni Holzmann, A. Romerosa Bernasconi, Steps ahead in understanding the catalytic isomerization mechanism of linear allylic alcohols in water: dynamics, bonding analysis, and crystal structure of an η²-allyl-intermediate, *Organometallics* 39 (2020) 4491–4499, <https://doi.org/10.1021/acs.organomet.0c00585>.
- [39] B. Lopez-Sanchez, A.B. Bohome-Espinosa, F. Scalambra, A. Romerosa, Ru complexes containing N-methyl-1,3,5-triaza-7-phosphaadamantane (mPTA) as catalysts for the isomerization of 2-cyclohexen-1-ol, *Appl. Organomet. Chem.* 37 (2022) e6971, <https://doi.org/10.1002/aoc.6971>.
- [40] B. Lopez-Sanchez, F. Scalambra, A. Romerosa, Transformation of the pheromone 3-methyl-2-cyclohexen-1-ol in the presence of RuClCp(PTA)₂ and [RuCp(OH)₂](PTA)₂CF₃SO₃, *Appl. Organomet. Chem.* 38 (2024) e7368, <https://doi.org/10.1002/aoc.7368>.
- [41] P. Servin, R. Laurent, M. Tristany, A. Romerosa, M. Peruzzini, F. Garcia-Maroto, J.-P. Majoral, A.-M. Caminade, Dual properties of water-soluble Ru-PTA complexes of dendrimers: catalysis and interaction with DNA, *Inorg. Chim. Acta* 470 (2018) 106–112, <https://doi.org/10.1016/j.ica.2017.04.044>.
- [42] A. Udvardy, M. Serrano-Ruiz, V. Passarelli, E. Bolyog-Nagy, F. Joó, Á. Kathó, A. Romerosa, Synthesis and catalytic activity of new, water-soluble mono- and dinuclear ruthenium(II) complexes containing 1,3,5-triaza-7-phosphaadamantane: Study of the effect of the visible light, *Inorg. Chim. Acta* 470 (2018) 82–92, <https://doi.org/10.1016/j.ica.2017.04.054>.
- [43] W.L. Ounkham, J.A. Weeden, B.J. Frost, Aqueous-phase nitrile hydration catalyzed by an in situ generated air-stable ruthenium catalyst, *Chem. Eur. J.* 25 (2019) 10013–10020, <https://doi.org/10.1002/chem.201902224>.
- [44] K.M. Vyas, P. Mandal, R. Singh, S.M. Mobin, S. Mukhopadhyay, Arene-ruthenium (II)-phosphine complexes: Green catalysts for hydration of nitriles under mild conditions, *Inorg. Chem. Commun.* 112 (2020) 107698, <https://doi.org/10.1016/j.inoche.2019.107698>.
- [45] A. Guerriero, M. Peruzzini, L. Gonsalvi, Synthesis of new ruthenium-CAP complexes and use as catalysts for benzonitrile hydration to benzamide, *Eur. J. Inorg. Chem.* (2021) 4669–4675, <https://doi.org/10.1002/ejic.202100743>.
- [46] M.C. Joseph, A.J. Swarts, S.F. Mapolie, Phenylacetylene polymerization mediated by cationic cyclometallated palladium(II) complexes bearing benzylidene 2,6-diisopropylphenylamine and its derivatives as ligands, *Dalton Trans.* 47 (2018) 12209–12217, <https://doi.org/10.1039/c8dt02728e>.
- [47] E. Bortolamiol, G. Isetta, I. Caligiuri, N. Demitri, S. Paganelli, F. Rizzolio, T. Scattolin, F. Visentin, Biological and catalytic applications of Pd(II)-indenyl complexes bearing phosphine and N-heterocyclic carbene ligands, *Eur. J. Inorg. Chem.* 26 (2023) e202300084, <https://doi.org/10.1002/ejic.202300084>.
- [48] a) R. Sahu, A.R. Kapdi, PTABS: A Unique Water-Soluble π-Acceptor Caged Phosphine, *Synlett* 34 (2023) 912–930, <https://doi.org/10.1055/a-1988-1861>;
- b) S.S.M. Bandaru, S. Bhilare, C. Schulzke, A.R. Kapdi, 1,3,5-Triaza-7-phosphaadamantane (PTA) Derived Caged Phosphines for Palladium-Catalyzed Selective Functionalization of Nucleosides and Heteroarenes, *Chem. Rec.* 21 (2021) 188–203, <https://doi.org/10.1002/ctcr.202000109>.
- [49] S.S.M. Bandaru, S. Bhilare, N. Chrysochos, V. Gayakhe, I. Trentin, C. Schulzke, A. R. Kapdi, Pd/PTABS: catalyst for room temperature amination of heteroarenes, *Org. Lett.* 20 (2018) 473–476, <https://doi.org/10.1021/acs.orglett.7b03854>.
- [50] S.S.M. Bandaru, S. Bhilare, J. Cardozo, N. Chrysochos, C. Schulzke, Y.S. Sanghvi, K. C. Gunturu, A.R. Kapdi, Pd/PTABS: low-temperature thioetherification of chloro (hetero)arenes, *J. Org. Chem.* 84 (2019) 8921–8940, <https://doi.org/10.1021/acs.joc.9b00840>.
- [51] S. Bhilare, J. Shah, V. Gaikwad, G. Gupta, Y.S. Sanghvi, B.M. Bhanage, A.R. Kapdi, Pd/PTABS: An Efficient Catalytic System for the Aminocarbonylation of a Sugar-Protected Nucleoside, *Synthesis* 51 (2019) 4239–4248, <https://doi.org/10.1055/s-0039-1690190>.
- [52] S. Bhilare, S. Kori, H. Shet, G. Balaram, K. Mahendar, Y.S. Sanghvi, A.R. Kapdi, Scale-Up of a Heck Alkenylation Reaction: Application to the Synthesis of an Amino-Modifier Nucleoside ‘Ruth Linker’, *Synthesis* 52 (2020) 3595–3603, <https://doi.org/10.1055/s-0040-1707260>.